Experimental and Numerical Assessment of Crashworthiness Properties of Composite Materials: A Review

aerospace

MDPI

Review

Experimental and Numerical Assessment of Crashworthiness Properties of Composite Materials: A Review

Maria Pia Falaschetti [1,2,*], Francesco Semprucci [1,2], Johan Birnie Hernández [1] and Enrico Troiani [1,2]

[1] MaSTeR Laboratory, Department of Industrial Engineering (DIN), University of Bologna, Via Fontanelle 40, 47121 Forli, FC, Italy; francesco.semprucci2@unibo.it (F.S.); johan.birnie2@unibo.it (J.B.H.); enrico.troiani@unibo.it (E.T.)

[2] CIRI Interdepartmental Center for Industrial Research on Aerospace, CIRI-Aero, University of Bologna, Via Baldassarre Carnaccini 12, 47121 Forli, FC, Italy

* Correspondence: mariapi.falaschetti2@unibo.it; Tel.: +39-0543374421

Abstract: Crashworthiness is a critical property that enables aerospace structures to minimise injuries and equipment damage during impact scenarios. This review examines the current state of crashworthiness research, with a focus on regulatory frameworks, experimental testing, and numerical modelling techniques. Stringent safety standards set by the Federal Aviation Administration (FAA) and the European Union Aviation Safety Agency (EASA) guide the design and certification protocols for aeronautical structures. Experimental crash testing, which includes both full-scale and subscale impact tests, provides essential data for validating material behaviour and energy absorption capabilities under both quasi-static and dynamic loading conditions. Advanced numerical modelling tools offer significant insights into crash behaviour, enabling optimisation of structural designs whilst reducing reliance on costly physical testing. This review highlights the integration of regulations, empirical data, and computational tools in advancing crashworthiness research, with an emphasis on developing safer, more efficient, and sustainable aerospace designs. Future directions should prioritise the use of sustainable materials and optimise crashworthy designs through artificial intelligence (AI) and advanced numerical models to enhance structural performance and safety.

Keywords: crashworthiness; composites; impacts; aerospace

Academic Editor: Kyungil Kong

Received: 29 December 2024
Revised: 23 January 2025
Accepted: 27 January 2025
Published: 6 February 2025

Citation: Falaschetti, M.P.; Semprucci, F.; Birnie Hernández, J.; Troiani, E. Experimental and Numerical Assessment of Crashworthiness Properties of Composite Materials: A Review. *Aerospace* **2025**, *12*, 122. https://doi.org/10.3390/aerospace12020122

1. Introduction

Crashworthiness is the ability of a structure to absorb and dissipate energy during a crash, thereby protecting passengers and cargo. This property is particularly vital in aerospace, where safety, performance, and weight efficiency are critical considerations. Modern aircraft are designed not only to withstand operational loads but also to mitigate the effects of catastrophic events through advanced materials, innovative structural designs, and advanced simulation techniques.

In aerospace history, different materials have been used to manufacture aircraft and helicopters aiming to meet stringent requirements for strength, weight efficiency, energy absorption, and durability. Since the advent of the first aircraft, metallic materials have been the primary choice for constructing main structural components. As the risks and challenges associated with impact scenarios became evident, these materials were also adapted for use in crashworthy designs, which began to be systematically implemented in both passenger and cargo vehicles to enhance safety during crashes. The most commonly used metals in aerospace applications are aluminium alloys, which are lightweight, ductile, and highly

suitable for structural components such as fuselage frames. Their ability to undergo plastic deformation during impact makes them quite effective for energy absorption. Recent advancements in materials technology have also introduced titanium alloys, with their exceptional strength and corrosion resistance. Whilst titanium alloys are not typically used in crashworthy components due to their low energy absorption capacity, they play a critical role in ensuring the structural stability of primary load-bearing elements during a crash. Another significant class of metals widely used in the aerospace industry is steel. Known for its high toughness and reliability under extreme conditions, steel is commonly employed in components where these properties are essential, such as the landing gear. However, its considerable weight with respect to aluminium limits its application to situations where strength and durability are necessary.

In the last forty years, the aerospace industry has seen the introduction of advanced materials, such as composite materials. This class of materials allows the enhancement of the structural properties whilst reducing weight, leading to the possibility of a higher payload capability, higher endurance, and lower fuel consumption. Conversely, composite materials represent a significant advancement in the design of crashworthy components, having demonstrated the ability to achieve stable crushing behaviour whilst delivering high specific energy absorption values. Moreover, due to their tailoring flexibility, composite materials allow for performance optimisation by adjusting parameters such as layup configuration, thickness, and geometry. This design flexibility exceeds that of metals, making composite materials highly adaptable for enhancing crashworthiness in aerospace applications. Carbon fibre-reinforced polymers (CFRPs), glass fibre-reinforced polymers (GFRPs), and aramid fibre-reinforced polymers are among the composite materials that play the main role in the aerospace industry. However, new composite concepts are being developed and implemented to improve the structural energy absorption properties. For example, thermoplastic matrix composites (e.g., PEEK) have high impact resistance, whilst elastomers can be used as shock absorbers for passenger protection.

The increased use of composite materials in aircraft, such as the Boeing 787 and Airbus A350, has led to revisions in crashworthiness regulations. These regulations were originally developed for metallic structures by international aviation authorities, such as the Federal Aviation Administration (FAA) and the European Union Aviation Safety Agency (EASA). Both the FAA's and EASA's airworthiness regulations contain comprehensive frameworks for crashworthiness standards in both fixed-wing aircraft and helicopters, aligning with their primary objectives but tailoring in their respective regulatory environments. Composite structures, with their unique failure modes and energy absorption characteristics, led to the introduction of special conditions (SCs) by the EASA and FAA to address gaps in the existing regulations. Complementing these efforts, CMH-17 (formerly MIL-HDBK-17) provides standardised methodologies for composite material design, testing, and crashworthiness. These evolving regulations and methodologies highlight a continuous effort to enhance crashworthiness, integrating technological advancements and ensuring safety across diverse aviation contexts.

As defined by these airworthiness regulations, experimental testing is essential for evaluating the crashworthiness of aerospace structures and ensuring passenger safety during crash events. Although standardised tests assess damage resistance and residual strength, they do not evaluate crashworthiness directly. To date, and to the authors' knowledge, there are no standardised tests that specifically measure the crashworthiness of composite materials. This lack of established standards highlights the uncertainties associated with composite behaviour in the aerospace industry. Consequently, this gap introduces risks, increases costs, and creates innovation barriers, ultimately resulting in application requirements that fail to fully leverage the potential of composite materials.

For instance, the EASA and FAA regulations stipulate that composite structures must withstand structural loads under impact conditions and that any damage incurred should not worsen under operational fatigue loads. However, without established crashworthiness standards, the certification processes for composite structures are often handled on a case-by-case basis. This approach leads to significantly higher costs and longer development timelines. Moreover, these rigorous requirements frequently result in thicker structures, which diminishes the advantageous strength-to-weight and stiffness-to-weight ratios offered by composites. A deeper understanding of composite behaviour could unlock the full potential of these materials in aeronautical applications, which is the motivation behind the numerous studies on this topic.

The absence of clear guidelines and design criteria poses significant challenges for the development of novel aircraft built with composite materials. Establishing internal evaluation protocols and conducting extensive test campaigns represents high costs, which many companies (i.e., start-ups) may find prohibitive. This financial burden limits innovation in the aerospace sector.

To assess crashworthiness, researchers employ various experimental setups to compare different materials and components, particularly crush tests, impact tower tests, and impact sledge tests.

Crush tests evaluate a component's energy absorption, failure modes, and load-bearing capacity under compressive loads, which could be quasi-static ($\leq$1 m/s) or dynamic (>1 m/s). Coupons for crush tests are categorised into flat plates (requiring an anti-buckling fixture) and self-supporting geometries, commonly including circular and square tubes, C-channels, corrugated panels, and hat sections. Dynamic testing can also be performed using impact towers. In this setup, a guided mass impacts the specimen at a controlled velocity. Conversely, impact sledges achieve higher energy and velocity impacts than impact towers, using a pneumatically accelerated device to strike the specimen.

Regardless of the experimental method used, many factors influence the crash behaviour of a composite structure, including material selection (matrix/fibre) and geometry (cross-sectional shape, configuration, thickness, and free length), trigger mechanisms, and stacking sequence. Researchers have, therefore, introduced various parameters to facilitate comparison across studies, i.e., energy absorption and specific energy absorption.

All the parameters affecting the crashworthiness properties of a component must be considered during the design and certification processes. However, assessing the influence of all these parameters through experimental tests is very costly. Therefore, numerical simulations have become essential, significantly reducing the reliance on experimental testing. Nevertheless, the complexity of composite materials introduces unique challenges. Unlike metallic structures, composites exhibit different failure mechanisms, including fibre fracture, matrix cracking, fibre–matrix debonding, delamination, and debris accumulation.

Capturing these behaviours and their effects requires advanced modelling techniques tailored to the unique properties of composite materials. These can be applied at various scales, each offering specific advantages and limitations. The mesoscale models are widely used, concentrating on ply-level interactions and interlaminar effects. They effectively bridge the gap between macroscale models, which focus on global structural response, and microscale models, which represent fibre–matrix interactions. Through the use of these numerical methods and the implementation of failure and damage criteria, it is possible to optimise the crashworthiness properties of a component by studying the trigger mechanisms' and geometry's influence in controlling failure progression and energy absorption. Moreover, numerical simulations allow the study of complex geometries, various stacking sequences, different trigger designs, and even the simultaneous use of integrated and

external triggers, which would be extremely costly and time-consuming if conducted solely through experimental methods.

This review aims to provide a comprehensive analysis of crashworthiness in aerospace, focusing on the evolution of materials, testing methodologies, numerical tools, and future directions. By synthesising insights from regulatory, experimental, and computational perspectives, this work highlights pathways for developing safer, more efficient, and sustainable aerospace structures.

2. Airworthiness Regulations

Regulations for crashworthy structures started to gain importance in the early 1960s after a series of studies on rotary and fixed-wing aircraft accidents between 1960 and 1965. These studies were primarily focused on occupant survival considering crash forces, structural failures, crash fires, and injuries [1]. Considering these studies, the U.S. Army presented the Crash Survival Design Guide (TR 67-22) in 1967 and then revised it in 1989. The guide is divided into five volumes [2] taking into consideration design criteria, checklists, crash environment, human tolerance to impact, occupant environment, test dummies, accident information retrieval, crash load estimation, structural response, fuselage and landing gear requirements, rotor requirements, ancillary equipment, cargo restraints, structural modelling, operational and crash environment, energy attenuation, seat design, litter requirements, restrain system design, post-crash fire, ditching, emergency escape, and crash locator beams.

The Crash Survival Design Guide was the foundation for the development of military standard MIL-STD-1290A for Light Fixed and Rotary Wing Aircraft Crash Resistance. Originally issued in 1974, it establishes the minimum crash resistance criteria that must be considered during the design phase, taking into account different impact conditions (impact direction, velocity, and object to impact) and survivability design factors. Technological advancements in rotorcraft design led to the discontinuation of this standard in the mid-1990s, allowing for greater design flexibility for contractors. Later, in 2006, it was reinstated without any revision due to its relevance for military programs [3].

Currently, aviation regulations in Europe are dictated by the EASA through Certification Specifications (CSs), which serve as non-binding standards outlining the means to demonstrate compliance with regulation (EU) 2018/1139 [4]. Some of these certification standards specifically address crashworthiness for specific categories: CS-23 for small transport aircraft, CS-25 for large transport aircraft, CS-27 for small rotorcraft, and CS-29 for large rotorcraft. For aircraft, the EASA's regulations address crashworthiness for the structural integrity of the cabin, fuel system safety, and emergency evacuation. In the case of rotorcraft, rotor and overhead protection are also considered. These regulations are constantly under review and updated as needed, with amendments aiming at enhancing safety by incorporating the latest technological advancements and improving the certification process. For instance, CS-25 was updated with Amendment 28 in December 2023. This amendment introduces a new structural ditching analysis in response to the emergency ditching of the U.S. Airways Flight 1549 in the Hudson River on 15 January 2019 [5].

In the United States, the FAA describes crashworthiness requirements under the Code of Federal Regulations (CFR). Specifically, Title 14 focuses on Aeronautics and Space. Crashworthiness is addressed in the following parts: Part 23 for Normal Category Airplanes, Part 25 for Transport Category Airplanes, Part 27 for Normal Category Rotorcraft, and Part 29 for Transport Category Rotorcraft. These regulations address various aspects of crashworthiness. For aeroplanes, Part 25 provides more detailed requirements, divided into three categories: structures (i.e., durability), design (i.e., emergency conditions), and design and construction (i.e., occupant physical environment). For rotorcraft, the same division

applies, but there is a special focus on vertical loads and crash conditions, which involve more unpredictable and dynamic scenarios due to the presence of the rotor. Analogous to the EASA, the FAA updates its regulations through Amendments; one example of recent updates related to crashworthiness is Cabin Interior Crashworthiness in Part 25 [6].

The increasing use of composite material in aircraft structures, exemplified by the Boeing 787 and the Airbus A350, both composed of more than 50% in weight of composite materials, has prompted significant changes to crashworthiness requirements in the existing regulations. The distinct failure modes and energy absorption characteristics of aircraft mostly made from this type of materials have led to significant changes in the design, verification, and certification processes for civil aircraft. To cover the gaps in the existing regulations, both the FAA and EASA have issued several special conditions (SCs). These SCs apply to specific aircraft or features and serve as additions or modifications to current regulations to adjust to state-of-the-art technology, including the novel materials used in the aforementioned aircraft [7]. For example, the EASA's SC C-01 [8] covers Crash Survivability for CFRP Fuselage (specifically for Airbus A350-941). Additionally, the FAA's SC 25-362-SC [9] outlines the crashworthiness of the Boeing Model 787-8 Airplane. In October 2023, SC No. 25-841-SC was published for the newest Boeing 777-9, which was still under development at the time of this publication. This standard covers Part 25 of the regulations, including modifications for Passenger Seats with Pretensioner Restraint Systems [10].

To further enhance the safety of composite material structures, the EASA released an Acceptable Means of Compliance (AMC) 20-29, applicable for CS-23, CS-25, CS-27, and CS-29 [11]. Similarly, the FAA issued an Advisory Circular (AC) 20-107B, which is relevant to Parts 23, 25, 27, and 29 of Title 14 [12]. Both documents provide guidelines to ensure that composite structures in aircraft meet the safety requirements, especially for crashworthiness and damage tolerance. In addition, both discuss repair and maintenance practices, testing and analysis methods, and manufacturing processes.

Another organisation dedicated to standardising methodologies for the processing, design, testing, and analysis of composite materials, including data development, is CMH-17 (formerly known as MIL-HDBK-17). Originally a military handbook, it has evolved over the years to address civilian applications, particularly in the aerospace and automotive sectors [13]. Its origins date back to 1943 with the release of the ANC Bulletin 17 "Plastics for Aircraft", which aimed to assist in the design of military and commercial aircraft containing polymeric materials. This bulletin addressed the mechanical and physical properties, moulding, and fabrication techniques of these materials due to their increasing importance at that time [14]. In 1959, the first MIL-HDBK-17 titled "Plastics for Air Vehicles" was published, utilising the content from the ANC Bulleting 17.

In 1978, a coordination group comprising members from the U.S. government, industry, and academia was established to work together to standardise composite materials' use. This effort led to the publication of MIL-HDBK-17B in 1988. Additionally, the group collaborated with the ASTM committee D-30, which focused on developing standard test methods, practices, terminology, and guides for composite materials [15].

In 2006, the sponsorship of the group moved from the U.S. Army to the FAA, reflecting a shift toward broader civil applications. Crashworthiness is addressed in CHM-17 and aligns with the EASA's and FAA's regulations. This topic was formally introduced in Chapter 16, Volume 3B of Revision G, released in 2012 [16]. This chapter, titled Crashworthiness and Energy Management, provides an overview of key factors that influence crash response. It includes design considerations and guidelines, manufacturing considerations, and test standards. The chapter outlines experimental guidelines, along with numerical and analytical predictive methods, and shares best practices to evaluate crashworthiness. Additionally,

it contains a description of material and structural responses, with a review of methods (experimental, numerical, and analytical) used by both industry and academia to characterise the crashworthiness properties at different scales, including successful examples of crashworthy designs [17]. It also discusses certification and compliance methodology guidelines for a comprehensive crashworthiness assessment.

3. Crashworthiness Parameters

No standard has been established to consistently characterise crashworthy structures. Consequently, comparison and evaluation across multiple studies are often challenging; however, to facilitate comparisons of different crashworthiness behaviours, several parameters have been introduced.

The principal outputs of tests to characterise crashworthiness are energy absorption (EA) and specific energy absorption (SEA). EA is defined as:

$$EA(x_c) = \int_{x_0}^{x_f} f(x)dx \tag{1}$$

where x_0 and x_f represent the initial and final crush displacement values considered for the calculation, x_c is the total crushed distance ($x_f - x_0$), and $f(x)$ is the sustained crush force.

SEA is considered a structural characteristic rather than just a material property, and it is influenced by various factors, including the composition of the material (i.e., fibres and matrix), the layup configuration, the geometry of the coupon, the loading fixture, and the crushing velocity. Furthermore, it does not consistently scale with changes in geometry [18,19]. It is calculated as:

$$SEA(x_c) = \frac{\int_{x_0}^{x_f} f(x)dx}{m\left(x_f - x_0\right)/h} \tag{2}$$

where m and h are the specimen's weight and length, respectively.

Other parameters are also used to compare different works, such as Crush Efficiency:

$$CE = \frac{F_{avg}}{F_p} \tag{3}$$

where F_{avg} and F_p are defined as the average force and the peak force (Figure 1). CE can be expressed as a percentage, so the formulation becomes:

$$CE_{\%} = \frac{F_{avg}}{F_p} * 100 \tag{4}$$

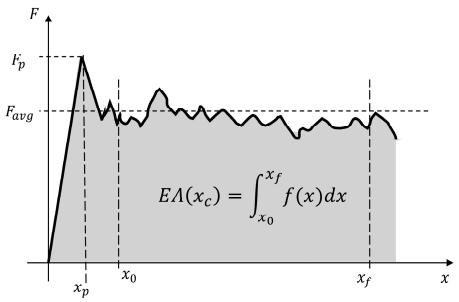

Figure 1. Example load–displacement chart for a crash test: x_0 is the initial crush displacement, x_f is the final crush displacement for the calculation of EA, x_c is the total crushed distance, x_p is the stroke at the peak, $f(x)$ is the sustained crush force, F_{avg} is the average force, and F_p is the peak force.

4. Experimental Methods for Crashworthiness Assessment

Experimental testing is essential for evaluating the crashworthiness of aerospace structures and ensuring the safety of the passengers during crash events. As specified in the previously discussed AMC 20-29 from the EASA, testing usually follows the "Building Block Approach", visually represented as a pyramid (Figure 2). This approach usually integrates experimental tests with analytical/numerical methods and varies the level of complexity, starting from simpler coupons and elements and advancing to complex structures over time.

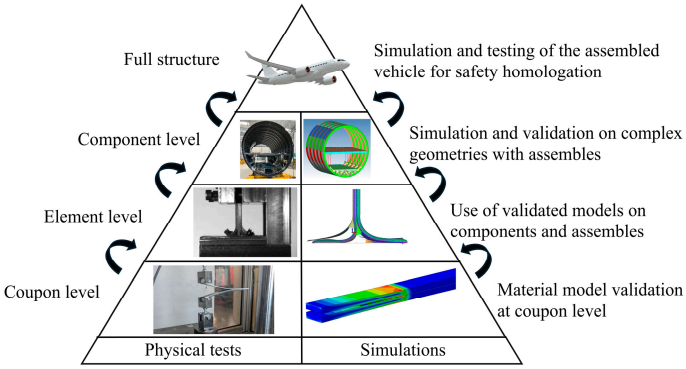

Figure 2. Building Block Approach pyramid scheme.

The base of the pyramid, comprising coupons and elements, requires a large quantity of tests. These tests are fundamental for the characterisation of the mechanical properties, energy absorption characteristics, and failure modes of the materials. Performing these tests at the beginning stage of a design process is essential to understand the behaviour of the material, to optimise the geometry, and to identify possible weaknesses at an early stage. In this manuscript, the tests necessary to study the crashworthiness behaviour at the coupon and element levels for composite structures are addressed.

There are several standardised tests for assessing the impact resistance of composite materials at the coupon level. These include, among others, the ASTM D7136, which measures the damage resistance of a fibre-reinforced polymer matrix composite during a drop-weight impact event; the ASTM D7137, which evaluates compressive residual strength properties; the ASTM D6264, which assesses the damage resistance of a fibre-reinforced polymer–matrix composite to a concentrated quasi-static indentation force; and the ASTM D6110, which examines the Charpy impact resistance of notched coupons and others to assess damage. These standards focus on evaluating the residual strength and damage after impact, but they do not directly assess the crashworthiness properties of a material or a structure. As of the publication of this manuscript, there are no standardised tests specifically designed to evaluate the crashworthiness behaviour of composite structures [20].

Different types of tests, however, have been developed to assess crashworthiness properties at the coupon or element level. The three main categories will be detailed in the following subsections.

4.1. Crush Test

These tests are designed to replicate crash conditions, where the specimen undergoes rapid compression to evaluate the energy absorption characteristics, failure modes, and load-bearing capability of a material. Key parameters, including the peak crushing load, average crush load, SEA, crush force efficiency, and others discussed in Section 3, are obtained from these tests. The results allow for the evaluation of the performance of a material, geometry, or structure to comply with safety standards.

Crush tests may be categorised based on the crushing speed (or loading rate), which can range from 1 mm/s up to 10 m/s. Up to 1 m/s, the test may be considered quasi-static [21]; in this case, the test speed is low enough to facilitate the study of failure mechanisms and energy absorption capability but may not accurately represent the properties of the material under real crash conditions since some may be strain-rate-sensitive [22]. The dynamic conditions (also found in the literature as "impact"), with a loading rate higher than 1 m/s, can replicate true crash conditions, where the crushing rate decreases from an initial velocity to rest due to the energy absorption. However, whilst dynamic tests provide realistic crash insights, they are challenging to analyse due to the high speed at which the event happens. Nevertheless, studies have highlighted the importance of performing this type of test [23–28].

Depending on the geometrical characteristics, coupons may be classified into two main categories: flat and self-supporting. Flat coupons (Figure 3a) are easy to manufacture but they need fixtures to avoid the global buckling issue [29]. For these, in fact, the critical buckling load is usually lower than the peak crushing load, making it difficult to characterise the crashworthiness characteristics of the coupon. One of the first fixtures was presented by Jackson et al. [30], who designed a fixture featuring guide rods, adjustable knife edges, and a sliding plate. This design was later modified by Lavoie and Morton [31], who implemented guideposts to improve the load transfer and increase the stroke. It was further modified by Feraboli [32], who adjusted the height of the knife-edge supports, avoiding the problems of tearing at the edges and preventing debris accumulation. Different designs were also proposed: Daniel et al. [33] modified the previously presented fixtures by eliminating the guide rods and substituting them with four support knife edges that accommodate different plate thicknesses and a loading bar; Jacob et al. [34] developed a design that incorporated a roller way as anti-buckling support and featured different contact profiles to isolate damage modes associated with frond formation. Lastly, it is worth mentioning the crush fixture developed by UK company Engenuity in consultation with the UK's National Physical Laboratory, the University of Utah, and CMH-17. This fixture is valuable for evaluating the various failure modes in both delamination-free and delamination-suppressed configurations, which is particularly important for numerical models focused on crashworthiness [35].

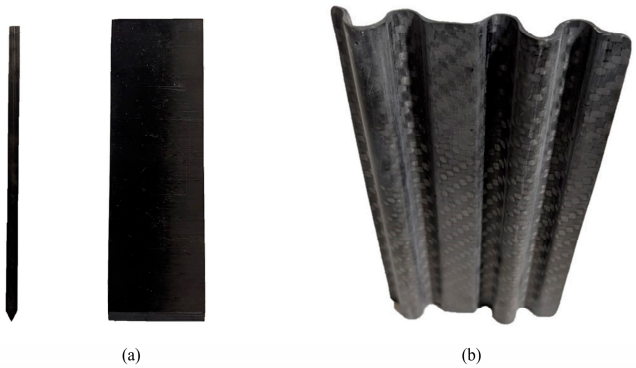

(a) (b)

Figure 3. An example of a flat coupon with the trigger (**a**) and a self-supporting coupon (**b**).

Conversely, self-supporting coupons are characterised by geometries that enable them to stand without any external help (Figure 3b) and resist instabilities when under a compressing crush load. Some may be potted into a resin base to improve their self-supporting stability during crushing, although this reduces their effective length [21]. Common geometries found in the literature include tubes (circular and square cross-sections), C-channels, corrugated shapes (low sine and high sine, semi-circular, circular), hat sections, and double-hat sections; all of these will be discussed in detail in Section 5.3.

The study of frictional effects during crush testing has been widely discussed since 1988 [36] when researchers first investigated the effect of sliding between the specimen and the testing plate. Over the years, considering flat coupons, the friction between the contact surfaces of the fixture and the coupon has also been analysed, indicating an overestimation of the crash force and SEA due to the energy dissipation caused by high friction [20,37,38]. Additionally, the triggering mechanism in crash coupons significantly affects test results and energy absorption [39]. Different types will be discussed in detail in Section 5.2.

4.2. Impact Tower

The impact tower test rig, also known as a drop tower, provides a cost-effective method to perform dynamic tests by impacting a specimen with a falling mass [40]. As seen in Figure 4, in this setup, a mass (g) is fixed to an impactor (d) at a predetermined height (h). The mass is released and guided by rails (f) to strike the specimen (b) at a certain velocity and energy. Accelerometers (e) are attached to the impactor to measure the acceleration during its descent and impact with the specimen, from which the force–displacement curve is obtained.

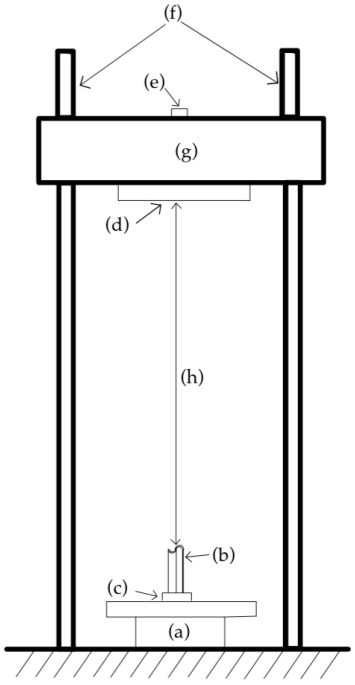

Figure 4. Drop tower set-up scheme, where (a) is the load cell, (b) is the coupon, (c) is the base fixture, (d) is the impactor, (e) is the accelerometer, (f) is the guide rails, (g) is the impact weight, and (h) is the free height.

Additional sensors, such as force sensors (load cells (a)) placed beneath the test specimen, optical sensors, or photogrammetry systems may be used to complement the data collected from the accelerometers (e.g., displacement) [41]. However, several challenges have been reported for this type of test configuration. These challenges include the incorrect interpretation of force–time curves due to inertial oscillations, unaccounted losses in kinetic energy resulting from inaccuracies in the preliminary setup calculations, and the overall calibration issues within the system [42,43]. This type of test rig also allows for performing non-axial impacts by placing the test on an inclined plane, which is preferred to the configuration where the impact is angled [40].

4.3. Impact Sledge

The impact sledge test rig, also referred to as the crash sledge test, can achieve higher energy and impact velocity when compared to the impact tower. Unlike the drop tower, this test is performed on a horizontal plane where the impactor is accelerated pneumatically at high pressure and guided by rails or tracks.

The specimen can be attached to the stopper or to the impactor. As stated by Haluza et al. [41], the instrumentation may vary; in addition to the usual load cells and accelerometers, to measure impact velocity, magnetic pickups, photo resistors, and laser-based velocimeters are used.

Moreover, for measuring displacement, options include potentiometers, laser-based velocimeters, and photogrammetry.

It is critical during post-processing to filter high-frequency noise, as it can interfere with important data, such as the peak crush load. To address this, a modal analysis of the whole test rig is needed to identify its resonance frequencies, which should then be filtered from the acquired data [44].

5. Key Factors

Several factors can influence the crush behaviour of a structure. The key considerations include the choice of the composite material constituents (i.e., matrix and fibres), as well as the structure's geometry. This comprises aspects like cross-sectional shape, overall configuration, thickness, and free length. Additionally, the design of trigger mechanisms, the incorporation of foam in sandwich structures, and fibre orientation are all critical elements. Each of these parameters significantly affects the structure's energy absorption properties and its deformation characteristics during an impact.

5.1. Material Constituents

Composite materials consist of fibres that provide reinforcement and a matrix that serves as the binding agent. In the most used composite materials, the matrix is a polymer matrix that can either be thermosetting, which offers rigidity and durability, or thermoplastic, which provides flexibility and reusability. The selection of fibre reinforcement is based on its specific mechanical properties, ensuring that it meets the requirements of the structure application effectively.

The selection of the polymer for the matrix significantly influences the specific energy absorption of composite coupons. Berry et al. [45] demonstrated that among thermosetting matrices, the SEA values ranked from highest to lowest as follows: epoxy, vinyl ester, polyester, and phenolic. This ranking was supported by the research by Thornton et al. [28] and Thornton and Jeryant [46], who observed the same SEA ranking: epoxy, polyester, and phenolic. Thornton noted that SEA did not appear to strongly correlate with the matrix fracture toughness. Instead, it seemed more influenced by the tensile strength and elastic modulus. Warrior et al. [47] supported these observations, demonstrating a similar hierarchy of SEA as that noted by Thornton. Whilst the tensile strength of the matrix had a good correlation with SEA, it was even stronger with the matrix compressive strength.

Ramakrishna et al. [48] conducted a comprehensive crush test study on thermoplastic matrix composite components. Their findings revealed that the SEA rankings of the materials tested listed from highest to lowest as follows: polyetheretherketone (PEEK), polyetherimide (PEI), polyimide (PI), and polyarylsulfone (PAS). This hierarchy was primarily attributed to the fracture toughness of the thermoplastic matrices, with PEEK having significantly higher fracture toughness than both PEI and PI. Additionally, PEEK samples exhibited a greater occurrence of fibre fractures, which, along with PEEK's crystalline structure (in contrast to the amorphous structure of PEI and PI), may enhance fibre bonding.

Hamada et al. [49,50] further compared carbon fibre/PEEK and carbon fibre/epoxy tubes, finding that when stable crushing occurred, SEA values were considerably higher for PEEK-based tubes.

In general, thermoplastic matrices tend to exhibit higher SEA values than thermosetting matrices. However, dynamic SEA values for thermoplastics can decrease by more than 50% compared to quasi-static values [49]. This significant difference makes epoxy resins the preferred choice due to their more predictable behaviour across various conditions.

An important property strictly related to the matrix choice is the interlaminar strength. A low value of this property results in lower energy absorption. In recent years, to improve interlaminar strength, methods such as using z-pinning [51], stitching [52], and through-thickness reinforcement [53] have been studied, showing promising results. The influence of z-pinning on the crashworthiness of CFRP structures demonstrates significant enhancements in energy absorption and structural integrity. Compared to unpinned designs, z-pinned configurations improve SEA by up to 4.49% in optimal patterns, such as vertical banded designs, whilst simultaneously reducing the initial collapse load [51]. The stitching influence on tubular structures was analysed by Rabiee et al. [52]. Stitched specimens showed an increase in SEA up to approximately 15% compared to unstitched samples. Additionally, the presence of stitching reduced the likelihood of catastrophic failure by distributing stresses more evenly across the structure and enhancing the interlaminar shear strength. Falaschetti et al. [53] evaluated the influence of integrating rubbery nanofibrous interlayers on the crashworthiness of CFRP corrugated coupons. The study highlighted that in quasi-static compressive crush tests, 10 μm and 20 μm interlayer mats raised the SEA by approximately 8.2%, providing an optimal balance between toughness enhancement and structural weight.

The most commonly used fibres for energy-absorbing composite structures are carbon, glass, and aramid (Kevlar). Among these, carbon fibres are predominantly utilised due to their excellent mechanical properties compared to the others, which often results in better behaviour under crash conditions, especially in terms of SEA. For specific applications, hybrid composites represent a feasible option by maximising the strength of each material whilst minimising its weakness. To achieve this, different types of fibres can be combined, such as Kevlar and carbon fibres, either within the same layer or in a hybrid stacking sequence (e.g., interleaving carbon layers with Kevlar layers).

An example of the comparison between mono-material composites and hybrid laminates with the same epoxy resin matrix is found in [54], which studied two stacking sequence and their effects on the crashworthiness properties of self-supporting C-channel coupons (Figure 5).

The results shown in Figure 5 highlight the different energy absorption characteristics of the materials, which are strongly related to their structural responses. Carbon fibre coupons absorb energy through a continuous crushing process, maintaining a relatively stable load with minimal oscillations during this process. When failure occurs, it leads to the formation of small debris, caused by stiff carbon fibre cracks, which fall apart during the test [54]. Kevlar fibre coupons show a behaviour similar to elastic–plastic materials. When oriented at $\pm 45^{\circ}$, these fibres exhibit a metal-like folding mechanism, leading to periodic variations in the load–displacement curves. Unlike carbon fibres, which tend to disintegrate into debris, Kevlar fibres do not break apart but display periodic folding. Hybrid layups (carbon/Kevlar) absorb energy similarly to the carbon segment. Carbon layers experience continuous crushing and fragmentation, whilst Kevlar layers enhance the coupon's structural integrity, preventing carbon debris' disintegration.

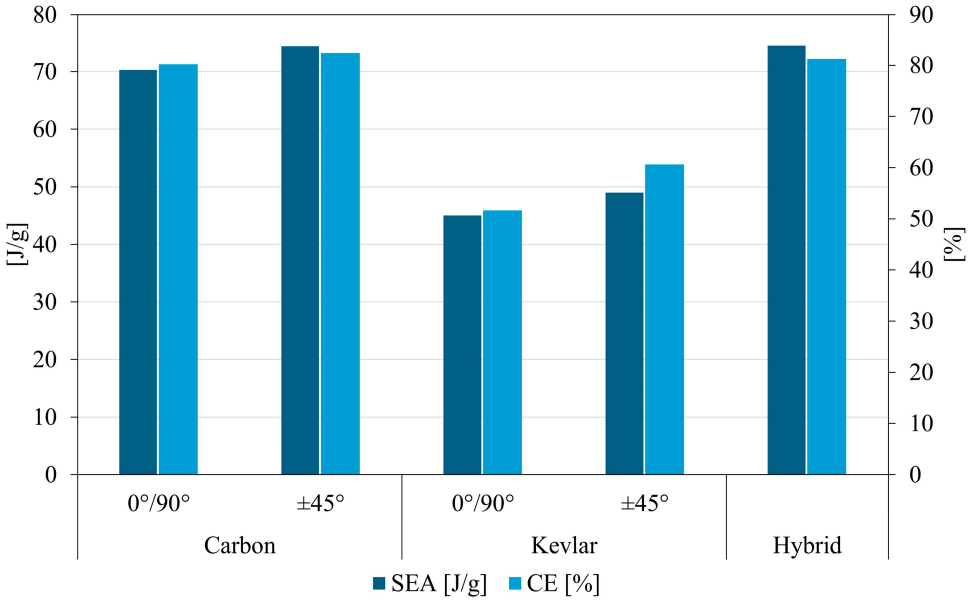

Figure 5. Crashworthiness properties comparison among carbon, aramid, and hybrid laminate.

Glass fibres are commonly used when the weight of the structure is not a critical issue, serving as an alternative to Kevlar laminates due to their comparable crashworthiness properties. In a study conducted by Guo K. et al. [55], the behaviour of corrugated coupons made with carbon fibres (CFs), glass fibres (GFs), Kevlar fibres (KFs), and their hybrid combinations was compared (Table 1). The study underlined the different behaviours of the various laminates: carbon fibres exhibited the highest SEA, whilst glass fibres provided moderate SEA. However, when combined with carbon fibres, glass fibres enhanced the overall SEA of the structures. Kevlar fibres offered a relatively high SEA and played a significant role in preventing catastrophic failure, performing well when hybridised with carbon fibre.

Table 1. Comparison among carbon fibre laminates (CF), Kevlar fibre laminates (KF), glass fibre laminates (GF), and their respective hybrids.

	Stacking Sequence	***SEA* (*J*/*g*)**
Single-Fibre Laminates	CF12	79
	KF12	42
	GF12	41
Double-Fibre Laminates	$[CF_3/GF_3]_s$	61
	$[CF_3/KF_3]_s$	56
	$[KF_3/CF_3]_s$	71
Triple-Fibre Laminates	$[CF/GF/KF]_{2s}$	51
	$[KF/GF/CF]_{2s}$	51

The double-fibre hybrid material combining carbon and glass fibres (CF_3/GF_3) exhibited the highest SEA among all double-fibre combinations, making it the most effective for energy absorption in this category. Conversely, the combination of Kevlar and carbon fibres $(KF_3/CF_3)_s$ achieved SEA values comparable to carbon fibre coupons, whilst providing a better failure mode. This combination helps to keep the material intact and prevents the carbon debris from dispersing. Combining carbon, glass, and Kevlar fibres in triple-fibre hybridisation results in balanced mechanical properties and high design flexibility. These combinations optimise energy absorption performance whilst avoiding catastrophic failure.

Additional strategies could be employed to enhance the crashworthy behaviour of composite structures, such as incorporating foams [56,57].

Özsoy et al. [57] studied the influence of expanded polypropylene foam on the crashworthiness of CFRP tube coupons, which had a diameter of 90 mm and a thickness of 2.2 mm. Polypropylene is a versatile material used in various applications, and its classification depends on its chemical properties and intended use. Depending on its formulation and curing process, polypropylene can function either as a matrix or a foam. This adaptability allows the polymer to be used in the form of expanded polypropylene (EPP), which can be specifically tailored for different functions, such as energy absorption in impact-resistant structures. The studied foam came in two different densities: 30 kg/m^3 and 60 kg/m^3, labelled as EPP30 and EPP60, respectively. The results from the study are summarised in Figures 6 and 7.

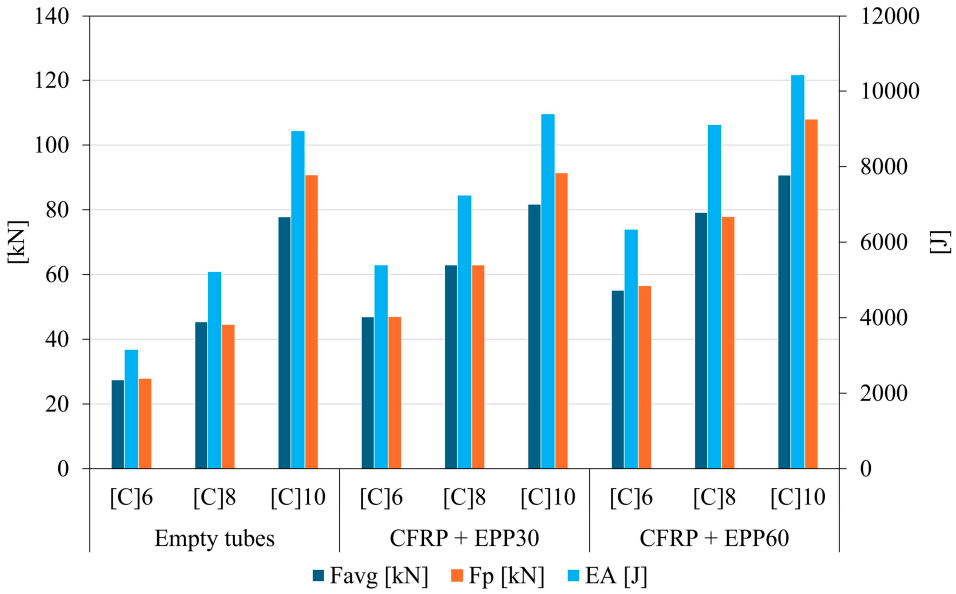

Figure 6. Average Force (F_{avg}), Peak Force (F_p) and Energy Absorption (EA) comparison among tubes filled with foam and empty tubes.

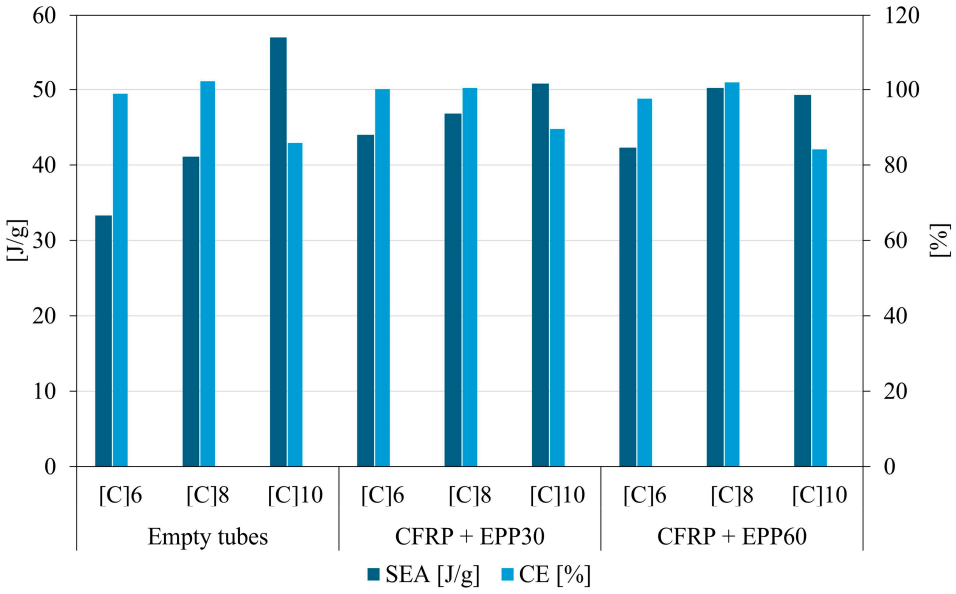

Figure 7. Specific Energy Absorption (SEA) and Crush Efficiency (CE) comparison among tubes filled with foam and empty tubes.

As shown, the effect of EPP foam filling on energy absorption behaviour and force distribution in CFRP tubes varies with the number of plies. In the case of eight-ply

CFRP tubes, the addition of the foam filling resulted in a progressive increase in SEA, demonstrating that foam reinforcement was more effective in these samples compared to others. However, for 10-ply CFRP tubes, the foam filling had the opposite effect, causing a decrease in SEA: the foam filling increased the amount of energy absorbed but the additional weight reduced the SEA efficiency, making it less effective compared to eight-ply tubes. For six-ply CFRP tubes, the highest SEA efficiency was achieved with 30 kg/m^3 EPP foam filling. Although the 60 kg/m^3 foam absorbed more energy, the added weight from the denser foam negatively impacted SEA, similar to the outcome observed with the 10-ply tubes. It is worth noting that the empty 10-ply CFRP tube absorbed approximately the same amount of energy as the 8-ply CFRP tube filled with 60 kg/m^3 EPP foam, yet it demonstrated a 14% higher SEA. This indicates that the number of carbon plies has a more significant effect on SEA than the presence of foam reinforcement.

In energy-absorbing structures, the goal of optimal design is to minimise the difference between peak force and average force. This approach helps prevent the transmission of excessive impact forces to the primary structure before the crash box undergoes deformation. Consequently, 6-ply and 8-ply CFRP tubes (both empty and foam-filled) would be a more favourable choice compared to the 10-ply component, showing peak forces approximately equal to the average forces.

5.2. Trigger

Among the various aspects influencing crash behaviour, the trigger mechanism plays a central role in initiating and controlling the progressive collapse of the structure. The failure trigger mechanism is of great significance in reducing the initial peak load, maximising energy absorption properties, and controlling the failure modes by introducing intentionally weak points in the structure.

These weak points are specifically designed to start the failure in a specific location and then direct the crushing along a predetermined direction, avoiding catastrophic failures and leading instead to a progressive failure (Figure 8).

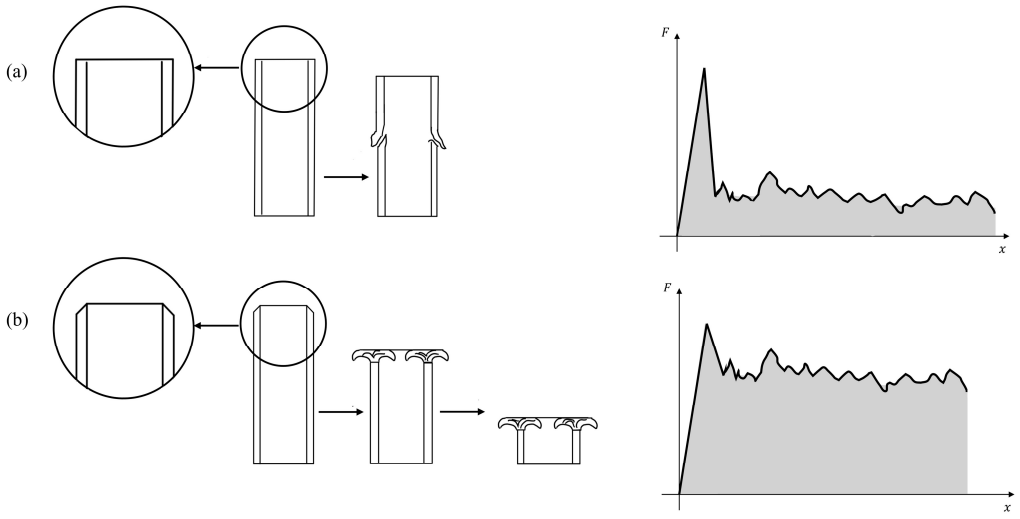

Figure 8. Effect of the trigger: (**a**) a coupon without the trigger (catastrophic failure) and (**b**) a coupon with the trigger (progressive failure).

Integrated triggers are typically obtained by either reducing the laminate thickness in specific areas [58] or incorporating localised cut-outs. Among these methods, localised cut-outs are frequently employed. Additionally, other mechanically induced triggers are used, including bevels or chamfered tips [59], steeple triggers [60,61], tulip triggers [62], sawtooth patterns [21], and ply-drops [63]. These can be manufactured either after the

curing cycle using machine tools or directly during the lamination process, properly cutting the plies to manufacture them [63].

Numerous studies have been carried out to assess the influence of the trigger design on the crashworthiness capabilities of a structure. Hussein et al. [64] conducted a study on cross-sectional square tubes, with a side length of 50 mm, with different triggers to evaluate their influence.

The tubes were manufactured from carbon/epoxy twill layers with an average total thickness of 2.1 mm. The triggers were then created on the tubes with different geometries. The first trigger was manufactured with four round tip notches (Figure 9a, labelled as CR4B), the second one with four sharp tip notches (Figure 9b, labelled as CS4B), and the last one with eight round tip notches (Figure 9c, labelled as CR8B). A 40 mm crush length was crushed, with a crushing velocity of 0.05 mm/s, producing the results depicted in Figures 10 and 11.

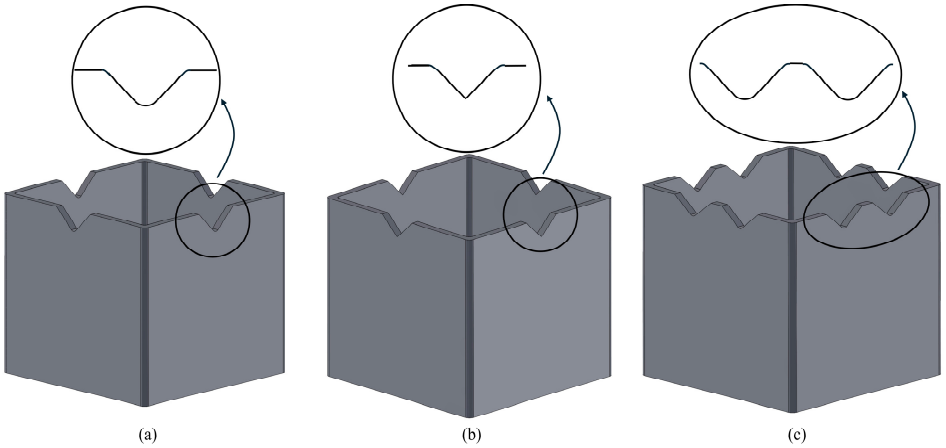

Figure 9. Three different trigger geometries: (**a**) 4 round tip blades, (**b**) 4 sharp tip blades, and (**c**) 8 round tip blades.

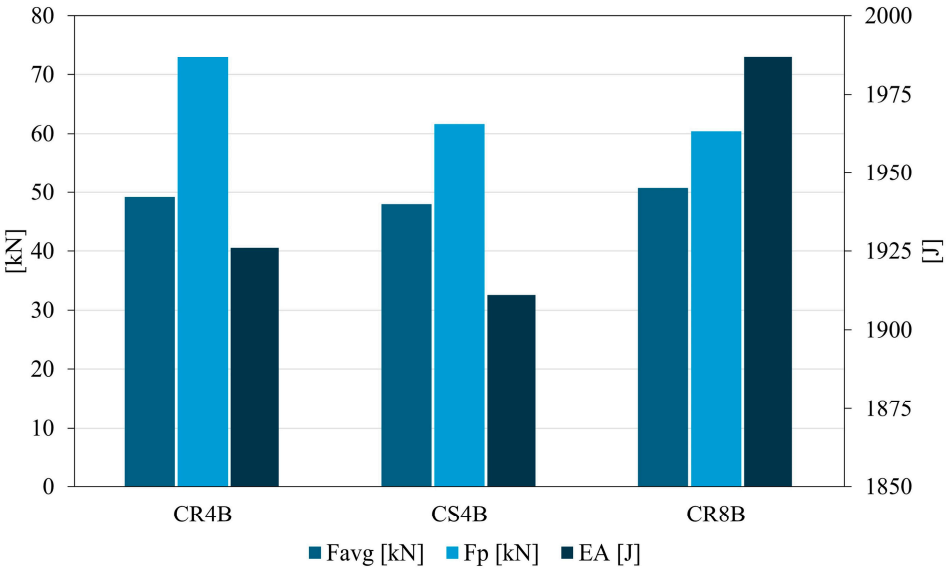

Figure 10. Average Force (F_{avg}), Peak Force (F_p) and Energy Absorption (EA) results of square tubes with different trigger configurations.

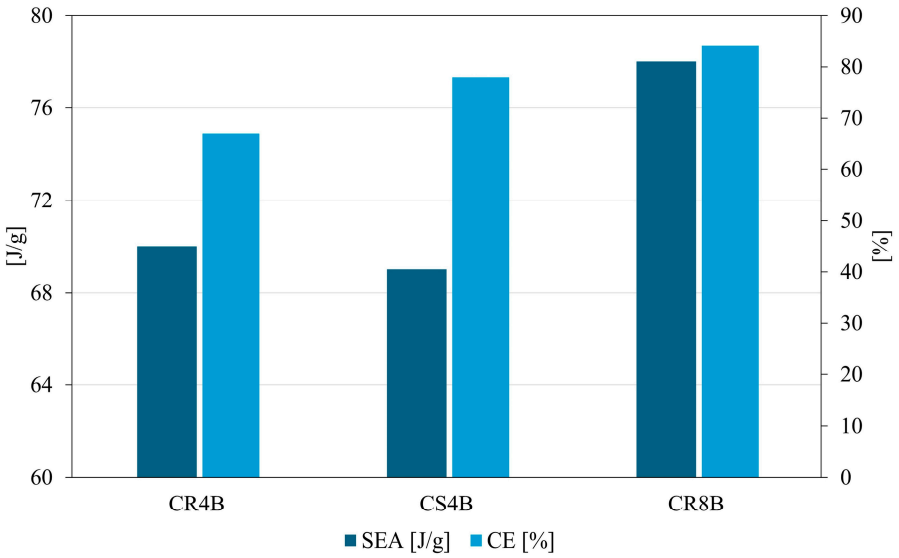

Figure 11. Specific Energy Absorption (SEA) and Crush Efficiency (CE) results of square tubes with different trigger configurations.

As ref. [64] demonstrated, the impact of this specific trigger geometry on SEA was minimal, with CS4B and CR4B showing nearly identical values. The most significant variation was observed in the peak force, which decreased by 15% when sharp-tipped notches were used. This change led to an 11% improvement in efficiency. Additionally, increasing the number of weakened points, as observed in the transition from CR4B to CR8B, led to a 17% reduction in peak force and a 3% increase in average force, thereby boosting efficiency by 17%. Concurrently, SEA exhibited a rise of approximately 10%.

Ma et al. [65] compared the influence of a single-bevel and double-bevel trigger (Figure 12) with various bevel angles on flat specimens (10 mm wide, 2 mm thick) manufactured with unidirectional carbon fibre with a polyamide matrix.

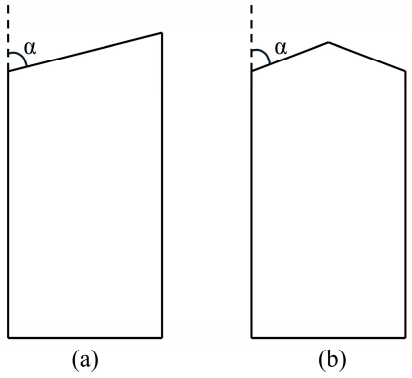

Figure 12. Coupon front view: single-bevel trigger (**a**) and double-bevel trigger (**b**); α is the bevel angle.

For single-bevel triggers, the peak load increased with the trigger angle, reaching a maximum value at 60°. The SEA followed a similar pattern, peaking at the same angle. Angles below 40° and above 70° exhibited unstable crushing behaviours, including local buckling or catastrophic failure, which significantly reduced energy absorption capabilities. Double-bevel triggers displayed a different trend, achieving a maximum peak load at 60°, a maximum mean load, and the highest SEA at 50°. Beyond 50°, the performance of double-bevel triggers dropped sharply, primarily due to increased buckling and delamination. Both trigger types showed their best crashworthiness characteristics at an angle of 60°, whilst outside the range of 40° to 60°, a reduced performance with lower energy absorption

and unstable fracture modes was observed. These results highlight the critical role of trigger geometry and angle in enhancing the crashworthiness of composite structures, with specific configurations yielding significant improvements in energy absorption and stability during the crushing process.

Huang et al. [66] evaluated the influence of the trigger mechanism in CFRP circular tubes with a 20 mm inner diameter through quasi-static crush tests (Figure 13). The study compared three different trigger geometries: a non-triggered coupon (Figure 13a), a ply drop-off trigger (Figure 13b), performed by gradually reducing the number of plies, resulting in a reduction in thickness for a portion of the specimen; and a self-adaptive trigger (Figure 13c), which was obtained by embedding shape memory alloy wires to a portion of the external surface of the specimen during the layup. The last one (labelled as SMA trigger) demonstrated superior performances, enhancing the SEA by 37.2% compared to the non-triggered coupon and by 22.8% with respect to those with a ply drop-off trigger. Similarly, the CE increased by 28.0% and 4.3%, respectively. Whilst the initial peak rose by 7.4% with the SMA trigger relative to the non-triggered coupons, the ply drop-off trigger caused an 8.9% reduction. This slight increase in peak force with the SMA trigger increased the SEA and CE without significantly compromising structural stability.

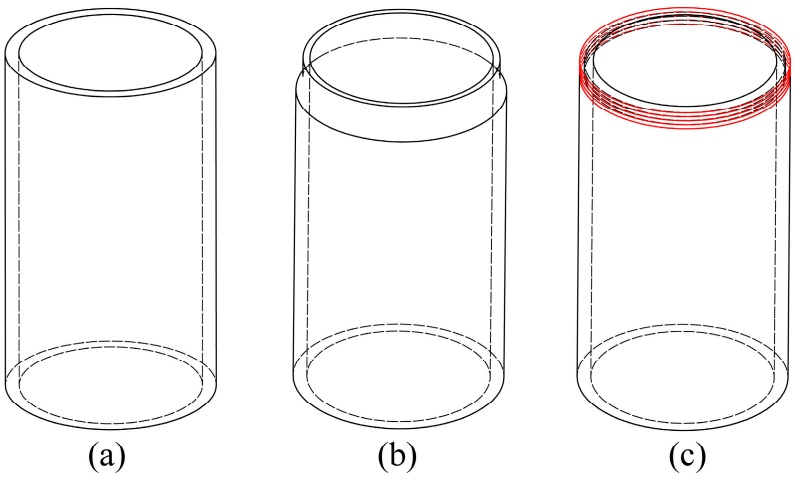

Figure 13. Comparison among different triggers: (**a**) no trigger, (**b**) ply drop-off trigger and (**c**) SMA trigger (SMA wires in red).

Moreover, the SMA trigger effectively constrained crack propagation, reducing the characteristic fracture length of lamina bundles and yielding a more stable and progressive crushing process. This contrasts with the behaviour observed in coupons without a trigger or those with a ply drop-off trigger, which exhibited more extensive delamination and less controlled failure modes.

All the studies underscore that optimising trigger design is pivotal for tailoring the mechanical response of crashworthy components, making them more effective in energy management during collisions whilst adhering to weight and material constraints in aerospace applications.

5.3. Cross-Section Geometry

A wide range of cross-sectional geometries are explored and employed in crashworthiness applications. These include both open-section geometries (such as flat panels [32,67–69], corrugated [70] or sinusoidal profiles [71], C-channels [21,72], and semi-circular shapes [70,73]) and closed-section geometries (including round tubes [44,74–76], square tubes [18,74,75,77], and double-hat configurations [78]). The geometry of a component is a key parameter for its crashworthiness performance, as energy absorption is

significantly influenced by the mechanisms of failure. Different geometries can result in different failure modes, with some being more advantageous for optimising energy absorption than others.

The impact of geometry extends beyond the cross-sectional shape; factors like the thickness and the length of the component are equally critical for crashworthiness applications.

Özsoy et al. [57] conducted a study to analyse the influence of the thickness of the geometry, i.e., of the number of layers, on the crashworthiness parameters. Circular cross-section tubes were produced using plain woven carbon fibre fabrics that were impregnated with an epoxy resin through a hand-layup process. Different stacking sequences were obtained with 6 plies ($[C]_6$), 8 plies ($[C]_8$), and 10 plies ($[C]_{10}$). The resulting tube thicknesses were approximately 1.32 mm, 1.75 mm, and 2.2 mm, with an inner diameter of 90 mm.

As Table 2 shows, SEA is strongly related to the number of plies. There is a 19% increase in SEA when the number of layers increases from 6 to 8, and a 28% increase when moving from 8 to 10 plies.

Table 2. Influence of the number of plies on the crashworthiness properties of circular cross-section tubes.

Coupons	Mass (g)	F_{avg} (*kN*)	F_p (*kN*)	EA (J)	SEA (*J*/*g*)	CE (%)
$[C]_6$	95.0	27.5	27.8	3160	33.3	98.9
$[C]_8$	127.0	45.4	44.4	5216	41.1	102.2
$[C]_{10}$	157.0	77.8	98.8	8945	57.0	85.8

Additional geometries, such as low-sine, high-sine, semi-circular cross-sections, and flat coupons have also been explored by Garattoni [79] and Feraboli et al. [80]. These studies underline the geometric effect on SEA (Table 3), demonstrating that the corrugated semi-circular geometry performs better.

Table 3. Comparison in terms of SEA among low-sine, high-sine, and semi-circular geometries.

Geometry	SEA (*J*/*g*)
Low Sine	52.5
High Sine	67.5
Semi-circular	70.0

Hu et al. [81] conducted a study on tube coupons produced using a woven glass cloth/epoxy prepreg intended for aeronautical applications. All tubes were manufactured with a layup configuration of $[\pm\theta]_{28}$, each having an internal diameter of 50 mm. The coupons were created with fibre orientations of $\pm15^\circ$, $\pm30^\circ$, $\pm45^\circ$, $\pm60^\circ$, and $\pm75^\circ$, maintaining a consistent wall thickness of 3 mm for all configurations. The study evaluated the impact of fibre orientation, obtaining the results shown in Figures 14 and 15. These show that the winding angle (θ) had a significant impact on the energy absorption capabilities of composite tubes. Specifically, the peak force experienced under quasi-static and impact conditions decreased as the winding angle increased from 15° to 45°. However, the peak force began to rise again with further increases in the angle, reaching up to 75°.

In quasi-static tests, the average force (F_{avg}) exhibited a pattern similar to the peak force (F_p), initially decreasing before rising again. However, the impact tests did not reveal a consistent trend; the tubes with angles of $\theta = 30^\circ$, 60°, and 75° showed relatively higher F_p, whilst the $\theta = 45^\circ$ tubes demonstrated the lowest value. The coefficient of efficiency first increased with θ from 15° to 60° and then decreased as θ rose to 75°, as observed under both quasi-static and impact conditions. Conversely, SEA showed no consistent trend with changes in θ. However, tubes with an angle of 45° exhibited the lowest SEA, whilst those

with 30° and 60° showed relatively higher SEA values in both testing conditions. The high crushing speed observed during the impact tests resulted in an increase in F_p values, whilst F_{avg}, CE, and SEA experienced a decrease. This indicated a lower energy absorption efficiency under dynamic conditions compared to quasi-static loading scenarios.

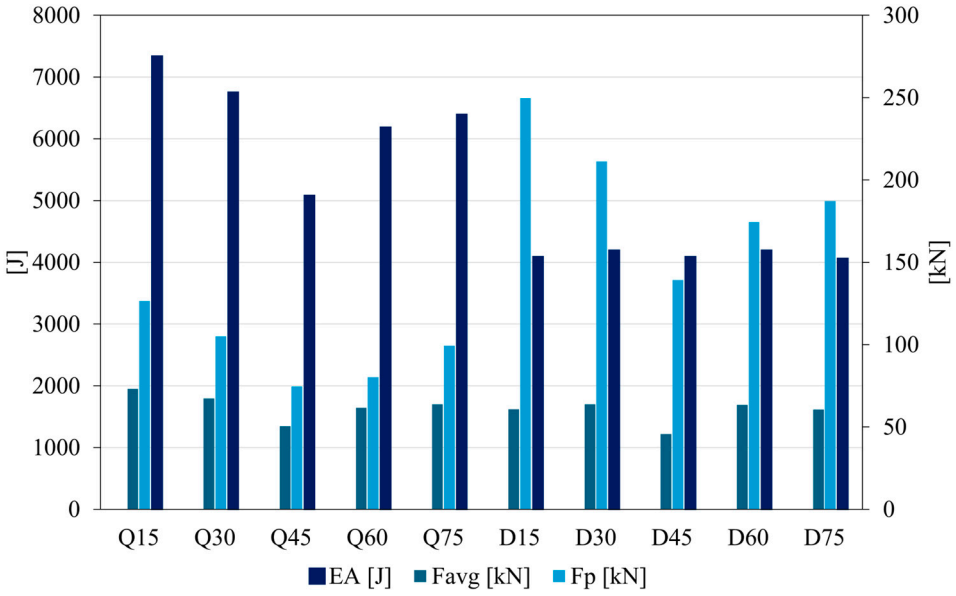

Figure 14. Fibre orientation effect on the Energy Absorption (EA), Average Force (F_{avg}) and Peak Force (F_p), on both quasi-static (Q) and dynamic (D) tests.

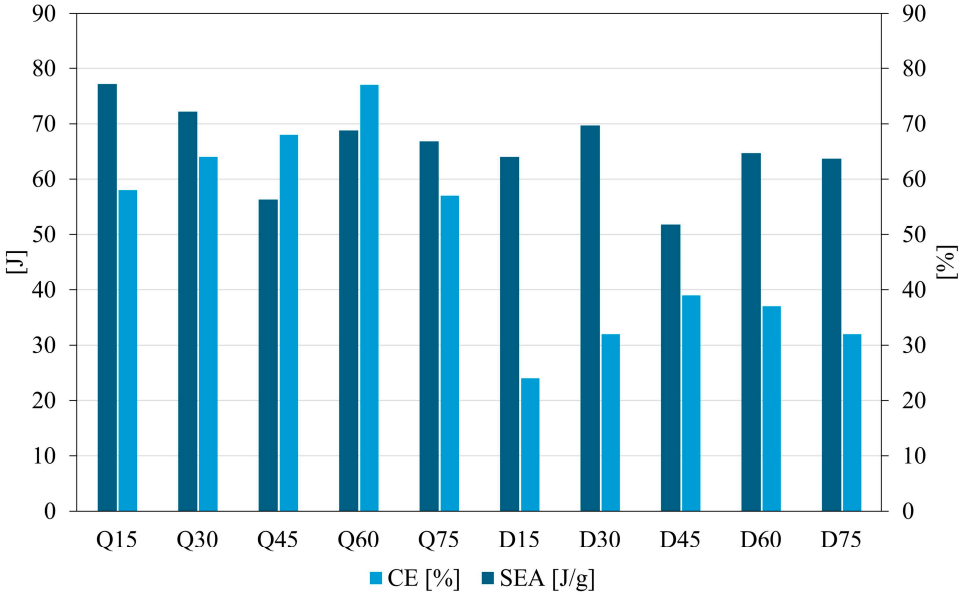

Figure 15. Fibre orientation effect on the Crush Efficiency (CE) and Specific Energy Absorption (SEA), on both quasi-static (Q) and dynamic (D) tests.

The results from the studies presented in this section (summarised in Table 4) highlight how the geometry, material, and trigger mechanisms of specimens affect the crashworthiness properties of composites. It is essential to combine these various parameters to achieve optimal energy absorption and controlled crushing.

Table 4. Summary of the material and geometry influence on *SEA*.

Geometry	Material	*SEA* (*J*/*g*)	Reference
Semi-circular	KFRP	49.0	[54]
	CFRP	74.4	
	GFRP	74.5	
Corrugated Semi-circular	CFRP	79.0	[55]
	KFRP	42.0	
	GFRP	41.0	
	CF/GF	61.0	
	KF/CF	71.0	
	CF/GF/KF	51.0	
	KF/GF/CF	51.0	
Circular Tubes	CFRP	57.0	[57]
	CFRP + EPP30 (foam)	50.8	
	CFRP + EPP60 (foam)	50.2	
Square Tubes	CFRP	78.0	[64]
Corrugated Low Sine	CFRP	52.5	[80]
Corrugated High Sine	CFRP	67.5	
Corrugated Semi-circular	CFRP	70.0	
Circular Tubes	CFRP	77.2	[81]

6. Numerical Modelling

Numerical simulations have become an essential tool in the structural design and certification of aerospace vehicles, particularly in crash analysis. These simulations enable engineers to reduce dependency on costly experimental testing during product design and certification stages.

For metallic structures, crash simulations have been highly effective in replicating ductile deformation and progressive folding mechanisms with minimal prediction errors [82–84]. However, modelling the crash behaviour of composite materials introduces unique challenges. Composite structures require detailed modelling of damaging processes that extend beyond the elastic region, encompassing failure initiation, propagation, and interactions between fibres and the matrix.

Composite materials exhibit a range of failure modes, including fibre fracture, matrix cracking, fibre–matrix debonding, delamination, and debris accumulation, often occurring across multiple length scales. Capturing these behaviours accurately requires detailed modelling tailored to the specific characteristics of the composite. To address this complexity, researchers employ different modelling approaches (macroscale, mesoscale, and microscale), each offering distinct advantages and limitations.

Due to the complexity of composite failure mechanisms, it is essential to define an appropriate length scale to accurately describe the material's characteristics [85].

Crashworthiness studies in composite materials generally involve three main modelling scales, i.e., macroscale, mesoscale, and microscale, each offering a different level of detail and suited for specific aspects of the material's behaviour.

6.1. Effects of Scale

Early modelling approaches primarily focused on global test characterisations performed at the macroscale (or structural scale). These models heavily depended on the overall laminate behaviour, simplifying the modelling process and significantly reducing computational time. However, this approach has notable limitations: it struggles to predict localised failure mechanisms, such as delamination or other specific damage modes.

Furthermore, critical parameters such as specific energy absorption and mean force cannot be reliably predicted, as these models rely heavily on data derived from structural-level tests rather than the fundamental mechanical properties of the material. Therefore, this approach is suitable for estimating global energy dissipation and broad damage patterns.

Conversely, the microscale approach aims to represent the complex physical phenomena occurring at the fibre and matrix levels. This method focuses on mechanisms such as fibre–matrix debonding [86], providing an in-depth analysis of the material's behaviour at the smallest scales. However, such detailed modelling requires an extensive set of physical parameters and internal variables for every type of damage mechanism [87], which are often difficult to measure or obtain experimentally. This approach offers unmatched insight into the underlying physical mechanisms, but it demands an exceptionally high computational effort, restricting its practical applications to fundamental research and material studies rather than to designing composite components or structures.

The mesoscale (ply-scale) approach bridges the gap between macro- and microscale modelling and is widely recognised as the most effective method for composite crashworthiness studies [88,89]. This scale corresponds to the thickness of individual plies and captures the interlaminar interactions between layers [90]. Compared to macroscale models, mesoscale simulations demand detailed constitutive laws but effectively balance computational efficiency with accuracy, providing a reliable representation of failure mechanisms. Mesoscale modelling has the advantage of accurately predicting a wide range of physical phenomena occurring at the crushing front, such as progressive failure modes and delamination [59,91]. This makes it particularly suitable for simulating composite structures at intermediate levels. Several numerical approaches have been developed to simulate the crushing behaviour of composite structures, each addressing different scales, aspects of energy absorption, and key material mechanisms.

6.2. Composite Material Models

Composite material models generally include three primary components: the elastic model, the failure criterion, and the post-failure damage model. The elastic model employs classical laminate theory to derive the stresses and strains within the laminate, based on the values obtained from the constituent lamina, as defined by the material model. The failure criterion serves to establish the point at which damage begins to occur. Finally, the post-failure damage model examines the progression of damage and the eventual failure of the material.

6.2.1. Failure Criteria

The development of failure criteria for composite materials has been a research topic since the 1960s, resulting in numerous theories available in the literature. These criteria can be classified based on several factors, including whether they are derived from strength or fracture mechanics theories, whether they offer a general prediction of failure or target specific failure modes, and whether they focus on in-plane or interlaminar failure.

Most failure criteria are applied at the composite ply level. Therefore, onset values such as strength or fracture toughness are closely related to structural properties and not to material properties, even though they are often referred to as the latter.

Due to their anisotropic nature, failure criteria for composite materials often specify distinct failure modes for both the fibre and the matrix. These failure modes are typically categorised based on different loading conditions, such as tension, compression, and shear, and may also include additional interactive criteria for complete ply failure. The two most commonly used criteria for assessing fibre and matrix failures are the maximum strain criterion and the maximum stress criterion.

When analysing fibre failure in tension, different criteria were proposed by Hashin [92], who used a quadratic interaction criterion involving in-plane shear; Chang and Chang [93], who incorporated a nonlinear shear behaviour into the previous method; and Puck and Schürmann [94], who used a maximum strain criterion with a stress factor applied to transverse stress. In compression, micro-buckling and kinking of the fibre during loading must be considered. This can be found in LaRC03 [95] and LaRC04 [96].

The criteria for matrix failure in tension usually consider a fracture plane in the transverse direction, involving an interaction between the tensile and the in-plane shear stresses. Aside from the maximum stress and maximum strain criteria, Hashin and Rotem [97] used a quadratic interaction criterion and Cuntze and Freund [98] used criteria based on the transverse tensile stress and strength and through-thickness shear stress. Further developments include nonlinear shear terms [93], in situ transverse tensile and shear strengths [99], crack density [100], and the use of plasticity laws [101]. For compression, Hashin and Rotem in [97] assumed that the fracture plane lies in the transverse direction and proposed a simple quadratic interaction criterion based on transverse normal and in-plane shear components. Hashin [92] extended this by including through-thickness strength, whilst Chang and Lessard [99] incorporated a nonlinear shear formulation. Cuntze and Freund [98] used only the transverse normal strength combined with several stress invariants. For criteria that account for a non-zero fracture plane angle, this angle must either be assumed or determined by evaluating all possible angles.

In other approaches for both fibre and matrix failure, different tension and compression ply properties are not specified; they are combined to obtain one criterion or not considered, as in Lee [102] or Christensen [103]. Other criteria, such as those in Tsai-Wu [104], Christensen [103], or Yamada-Sun [105], do not consider the separate ply failure modes. These criteria are more suited and applied whenever delamination can be ignored.

For delamination initiation, the criteria use the stress values of an individual ply or interface elements between plies, combining through-the-thickness tensile and shear characteristics [92,102]. Only a few consider the stress in the fibre direction [106]. Most criteria for predicting the growth of pre-existing delamination rely on the concept of fracture mechanics, specifically the strain energy release rate. This is combined with threshold toughness values in the mode I, II, and III openings.

To simulate delamination failure, a damageable layer (including either node-to-node bar elements or continuous elements) must be implemented between the composite plies. Typically, the interface element transfers all traction between plies until a specific criterion is met, after which the element's stiffness begins to degrade. This degradation continues until the interface reaches zero stiffness, at which point the substructures are completely separated. The interface element then functions solely as a contact region, preventing any unphysical crossover between the two substructures. The behaviour of the interface element is determined by the constitutional relationship (bilinear, exponential, or linear–exponential) between the relative displacement of the two connected plies and the traction generated between them due to damage mechanics. Benzeggagh and Kenane [107], Camanho and Dávila [108], Borg et al. [109], and Qiu et al. [110] are some examples.

6.2.2. Damage Models

In composite materials, the onset damage does not usually result in ultimate failure. Therefore, it is essential to define a damage model that progressively degrades the material's performance until ultimate failure occurs. Damage models for crashworthiness analysis are typically categorised into three primary groups: progressive failure models (PFMs), continuum damage models (CDM), and non-local damage models (NDMs). Each model type has unique characteristics and is suited for different applications.

PFMs are commonly used in large-scale simulations and involve the sequential elimination of finite elements as they meet predefined failure criteria (such as the Chang and Chang [93], Puck [94], or Tsai-Wu [104] criteria). These models operate by progressively degrading the material until complete element deletion occurs. However, PFMs oversimplify the complexities of crushing phenomena, particularly when simulating post-failure behaviours such as delamination or the fibre–matrix interaction. At the same time, their accuracy heavily depends on extensive calibration, requiring adjustments to numerical parameters to align with experimental results. PFMs are, therefore, best suited for applications where simplicity and computational efficiency outweigh the need for detailed material behaviour. An example could be identified in Hamada et al. [111], where a progressive crushing method was used to predict the mean crush load of composite tubes. It focused on the splaying mode, characterised by longitudinal cracking of the tube wall below the debris wedge. The model was found to be heavily dependent on geometry and limited in scope, as it addressed lamina bending and cracking solely.

CDMs offer a more detailed approach by incorporating material softening through internal variables that degrade mechanical properties. Damage is represented mathematically by introducing damage variables into the material's constitutive equations. These variables reduce stiffness progressively as damage evolves. CDMs have high fidelity in capturing the degrees of material failure compared to PFMs; moreover, they offer the possibility of representing the damage evolution processes, such as crack initiation and propagation, making this class of models suitable for midscale simulations where detailed behaviour is critical. However, despite their advantages, CDMs are computationally demanding, which makes them less practical for large-scale models without substantial computational resources. Some examples of this kind of model are Talreja [112], Johnson et al. [113], Ladevéze [88,114], Maimí et al. [115], and Sokolinsky et al. [59]. Each of these models introduces damage factors into the ply stress–strain equations, inversely affecting the material's constitutive properties. These factors degrade the ply stresses after failure, following the damage function defined by the material model. The analysis proceeds until the stress is fully degraded to zero or another specified condition for ultimate failure is met. Another example of a CDM was first developed by Matzenmiller et al. [116] and later improved by Williams et al. [117]. This model employs a homogenised continuum framework to establish the constitutive theory for anisotropic damage and elasticity. To capture the damaged state evolution under applied loads, internal variables are introduced, which subsequently account for the progressive degradation of material stiffness. The kinetic formulation is completed with evolution equations that describe the progression of the passive damage variables. McGregor et al. [118,119] then introduced damage propagation and energy absorption in the axial crushing of braided composite tubes in the model. The model used representative volume elements to capture the main characteristics of the material based on the physics of the composite behaviour.

Finally, NDMs bridge the gap between PFMs and CDMs by combining the scalability of PFMs with the detailed material behaviour modelling of CDMs. Unlike local models, which suffer from stress localisation at discontinuities, NDMs mark the effects of cracks over a defined region. This is achieved using traction–separation formulations, which distribute stress and strain gradients more realistically.

NDMs allow the scalability of large simulations without extensive recalibration, reducing the sensitivity to mesh size and element orientation and addressing issues of numerical instability. NDMs have gained increasing attention in recent years due to their versatility and their ability to handle multiscale phenomena, making them highly promising for advanced crashworthiness simulations accurately reproducing complex material behaviours

like crushing or fragmentation. Waas and Pineda [120], Bazant et al. [121,122], and Rabczuk and Belytschko [123] represent a few examples of this modelling methodology.

Some authors have also developed hybrid damaging models in order to balance computational costs and the accuracy of results. Examples include Lorentz and Andrieux [124], combining local damage variables with non-local regularisation, and Guguin et al. [125], where the micromechanics are combined with the non-local theories to account for fibre–matrix interactions and neighbouring ply effects during damage progression.

In other studies, different kinds of damage modelling have been proposed; for example, in the study conducted by Fleming [126], the Virtual Crack Closure Technique (VCCT) [127] was used to model the splaying delaminations that occur during the crushing of composites. This approach simulates the interaction between two sub-laminates connected by spring elements, allowing for the calculation of energy release rates based on nodal forces and displacements near the crack front. Whilst the VCCT offers a physically based framework for modelling delamination phenomena, it is highly sensitive to mesh refinement and depends on accurate dynamic property data, which may not always be readily available for generalised crash analyses. Fleming acknowledged that the technique's dependence on extensive characterisation makes it unsuitable as a predictive tool for crash modelling. Specifically, its applicability is limited by the need for calibration tailored to specific material and geometry combinations, reducing its practicality for extensive studies on crashworthiness.

6.2.3. Model Implementation Example

Many of the described models are nowadays implemented in commercial software, such as Radioss, Abaqus, LS-DYNA, and ESI-Virtual Performance Solutions, and numerous examples of their applications can be found in the literature.

One of the earliest model applications was proposed by Farley et al. [128], who implemented the maximum failure strain criteria to simulate interlaminar crack growth and the fracture of lamina bundles. Validation of the model with experimental results for aluminium, Kevlar/epoxy, and graphite/epoxy tubes demonstrated its versatility and accuracy.

In the early implementations of composite models, the material was often treated as a single shell, a simplification that failed to capture the true crash failure behaviour of composite components accurately. However, with advancements in computational capabilities, more detailed modelling approaches emerged, allowing for the simulation of the entire stacking sequence and a more realistic representation of the material's behaviour.

In [129], a laminate was modelled using a shell–beam element approach and the Ladevéze damage model. This method enhanced the stability of finite element (FE) models for crashworthiness simulations of thin-walled composite structures and improved the overall capability for through-thickness deformation of the element. This approach effectively addressed issues commonly encountered with traditional elements, such as instability and convergence problems, whilst maintaining the flexibility and efficiency of 2D discretised elements and the stability of 3D discretised elements.

The recent literature highlights the applications of the Ladevéze damage model, particularly in the work by Rondina et al. [58], where the fabric version of the model was used to evaluate the crashworthiness properties of corrugated self-supporting coupons. The study also compared the Ladevéze model with the Waas–Pineda model, emphasising their differing approaches. The laminate was discretised using shell layers to represent each ply, with cohesive elements in between to represent the interlaminar interfaces. Additionally, a sensitivity analysis of various parameters was conducted. Both models showed good agreement with the experimental data. Detailed information on the calibration methods for

both damage models, as implemented in ESI-VPS Visual Crash-PAM, can be found also in the work of Falaschetti et al. [130].

In Riccio et al. [131], a C-channel stanchion was modelled, implementing the Hashin failure criteria for the interlaminar damage and a specific continuum damage mechanics approach (stiffness degradation of the material after the failure onset governed by the material toughness) whilst the interlaminar damage was simulated by adopting the Cohesive Zone Model (CZM). The work showed a good agreement with the experimental results related to the test of a sub-floor support system in the cargo area of a commercial aircraft.

Examples of PFMs can be found in Feraboli et al. [132] or Raponi et al. [133], where the MAT54 of LS-DYNA was used to simulate the crashworthy behaviour of carbon/epoxy and Poly-Propylene-fibre/Poly-Propylene-matrix specimens, respectively. In both cases, Chang and Chang's failure model was implemented, whilst the post-failure progressive damage was realised through ply-by-ply failure within the laminate, and once all plies failed, the element was deleted. The results indicated that, although MAT54 can successfully simulate the experiment, several modelling parameters require calibration through a trial-and-error procedure. The same was assessed by Perfetto et al. [134], Caputo et al. [135] and Manzo et al. [136], who modelled the full-scale fuselage section of a regional aircraft made entirely of composite materials (thermosets and thermoplastics) under drop tower loading conditions. The simulations included the modelling of the fuselage external structures (skin, ribs, stringers), the floor and the crashworthy components designated to the impact energy dissipation, the mannequins representing the passengers, and sensors to measure the accelerations that the body would experience during a crash event.

In [137], Xiao et al. conducted a comparative study of the MAT58 and CODAM models in simulating the behaviour of braided composite tubes. The latter is a damage mechanics-based composite constitutive model developed at the University of British Columbia. The results revealed that MAT58 underestimated total energy absorption in simulations compared to experimental data, highlighting the need for modifications to its degradation law to better capture the behaviour of compressively damaged composite materials. In contrast, the improved CODAM model produced more accurate crush morphologies and demonstrated strong agreement with experimental results in terms of the force–displacement response and total energy absorption.

6.2.4. Trigger Modelling Techniques

As discussed in Section 5.2, trigger mechanisms are a fundamental part of initiating and controlling the progressive collapse of a structure. Modelling strategies for triggers directly affect the simulation's ability to replicate the real behaviour of the composite structures. Effective trigger modelling not only improves the fidelity of simulations but also guides the design of components to achieve optimal crash performance. Numerous studies in the literature focus on modelling methods for triggers.

Jiang et al. [138] conducted a comprehensive investigation into the effects of different geometric triggers on the crash performance of composite corrugated coupons. They compared triggers with varying designs, including chamfers at different angles, wedges, slanted, and straight configurations, focusing on key parameters such as initial peak load, sustained load, and specific energy absorption. Additionally, the study explored the influence of multi-angle bevel triggers. Among the tested designs, the 45° chamfer trigger demonstrated the best performance, achieving the highest sustained crush load, energy absorption, and SEA. The angle of the chamfer trigger had minimal influence on crashworthiness, except in the case of a 0° chamfer (i.e., no trigger), which obviously showed unwanted behaviour. The corrugated beam used in their work was modelled in Abaqus with stacked continuum shell elements and the CODAM damage model. In the simulations,

a convex trigger design combining 45° and 60° angles demonstrated enhanced crashworthiness properties. However, replicating this design through experimental manufacturing is not feasible, making this approach impractical for implementation.

Joosten et al. [60] adopted a stacking-shell/cohesive-element modelling approach implemented in ESI-VPS (at that time ESI PAM-Crash) to assess the different steeple trigger geometry effects. In particular, the fabric global composite ply (PLY7) [139] was used. The results showed that the steeple-type trigger is effective in preventing undesired failure modes thanks to the high stresses that generated delaminations and splaying. A development of the steeple trigger is the saw-tooth trigger, a repeating sequence of successive cut-outs along the width of the structure. It is usually used in flat coupons [140] but some examples could be found in different geometry components [138].

The ply-drop trigger geometry was investigated by Luo et al. in [141], where a solid 3D finite element model was implemented in Abaqus. Different trigger ply-drop methods were modelled on a corrugated beam. Whilst the numerical simulations accurately captured the steady-state behaviour of the experimental components, discrepancies were observed in the initial peak force. This indicated that the numerical triggering modelling did not fully replicate the experimental results.

Recently, researchers have investigated external triggering mechanisms designed to induce specific failure modes, such as a plug-type trigger. This type of trigger is integrated into the structure and is typically rigid. It restricts the deformation of the specimen in undesired directions, ensuring that the failure occurs in a controlled manner. Jiang et al. [142] conducted a numerical investigation of various plug trigger geometries. They found that a grooved design featuring ditches of varying widths could effectively reduce the initial load peak whilst maintaining a high sustained load, thereby enhancing the specific energy absorption. Later, Ren et al. [143] used the same plug trigger geometry and combined that with different integrated trigger methods (i.e., chamfer, holes, ply-drop, saw-tooth). The study showed that the ply-drop trigger worked more effectively when used alongside the narrow ditch plug. This combination resulted in the lowest initial peak load, a gradual increase in the crushing load, the highest average sustained load, and the least fluctuation in the curve. However, this performance can only be achieved if the buckling of the structure is prevented, which limits its application. All these studies emphasised the critical importance of incorporating a well-designed trigger to ensure accurate simulation results and to enhance the predictive reliability of crashworthiness simulations.

In summary, various numerical models have been developed to effectively predict the crashworthiness of composite structures. However, it is important to recognise the limitations of numerical simulations in these analyses. Each type of model captures specific material behaviours based on a set of assumptions, leading to the conclusion that no single model can account for all potential scenarios. Consequently, it is crucial to focus on the specific outcomes that each simulation can achieve.

There are additional limitations to consider, such as the simplifications made regarding material behaviour and boundary conditions. These simplifications influence computational costs and may fail to accurately represent the variability in real-world structures. For instance, complex geometries are often approximated to manage computational resources, which can potentially compromise the accuracy of the results. Moreover, accurately modelling phenomena such as strain rate sensitivity also presents challenges, while boundary conditions in simulations are typically simplified representations of real-world scenarios, affecting overall result fidelity.

High-fidelity models with detailed meshes are essential for accurately capturing complex deformations and interactions. However, such models require substantial computational resources and time. Nonlinearities, including large deformations and contact

interactions, further increase these requirements. Additionally, real-world variability in material properties, manufacturing tolerances, and assembly processes introduces uncertainties that simulations often fail to adequately represent.

Improvements can be made in several areas. Integrating microstructural details, such as fibre and void distributions, into material models can yield a more realistic representation of material behaviour. Techniques like adaptive mesh refinement can optimise computational resources by focusing on critical regions of the model, thus balancing accuracy and efficiency. Furthermore, meshless methods offer promising solutions for scenarios involving extreme deformations or fractures.

The adoption of advanced modelling techniques, such as multiscale and multi-physics modelling, can significantly enhance simulation accuracy. Multiscale modelling bridges the gap between the micro and macrostructural responses of a structure under crash conditions, providing a more comprehensive understanding of its behaviour. Meanwhile, multi-physics modelling improves accuracy by incorporating various physical phenomena, including thermal, fluid, and electromagnetic interactions, which are particularly relevant for emerging technologies like hydrogen-powered aircraft. Structural–thermal coupled crashworthiness simulations could play a critical role in assessing the performance of liquid hydrogen fuel tanks under extreme storage temperatures.

Machine learning techniques are increasingly being employed to enhance predictive capabilities and improve the reliability of numerical models. By analysing extensive datasets from both simulations and experimental studies, machine learning algorithms can identify complex behaviour patterns that might otherwise be overlooked, providing insights into the actual performance of structures. Machine learning can also identify discrepancies arising from model assumptions or simplification, facilitating the development or refinement of models to better predict real-world crash behaviours.

Advancements in solvers are equally crucial. The implementation of parallel computing and GPU acceleration can significantly reduce computation times, making large-scale models more feasible. Additionally, improved algorithms for handling contact and interaction during deformation can also enhance the accuracy of simulations involving complex structural behaviours.

7. Future Directions and Potential Research Areas

To enhance the crashworthiness of composite structures, future research should explore several innovative and multidisciplinary topics. Some of these include the following.

7.1. Advanced Materials

Materials like Dyneema, an ultra-high-molecular-weight polyethylene already utilised in high-performance applications such as America's Cup sailing competitions, offer significant potential for crashworthy applications. Dyneema combines exceptional ultimate tensile strength (3.3–3.9 GPa), elastic modulus (109–132 GPa), and low density (970–980 kg/m^3), making it a promising candidate for lightweight and energy-absorbing components. In addition to Dyneema, other advanced materials, such as graphene, could be explored for their extraordinary strength-to-weight ratios and adaptability in composite applications.

Thermoplastic matrices offer a promising avenue for developing reusable composite components, contributing to reducing the environmental footprint. Advanced materials such as polyetherketone (PEK), polyetheretherketone (PEEK), and polyethersulfone (PES) exhibit intriguing mechanical properties and have already been studied for specific crash structures [144]. Further research into these materials could enhance their optimisation and broaden their application in crashworthy designs. These thermoplastics combine durability with recyclability, addressing sustainability concerns whilst maintaining structural perfor-

mance. Further investigating their integration into crashworthiness design could lead to innovative solutions that balance safety, efficiency, and environmental responsibility.

7.2. Sustainability

As the aerospace industry increasingly prioritises the reduction in environmental impacts, natural fibres such as flax, ramie, and hemp have emerged as promising alternatives. These renewable materials exhibit mechanical properties comparable to traditional structural materials, making them viable candidates for crashworthy applications. Additionally, basalt, a natural mineral fibre, offers durability and high-temperature resistance, further broadening the scope of sustainable solutions.

However, the effective integration of these natural fibres into hybrid composites requires further research. Optimising their energy absorption capabilities whilst minimising their environmental impact presents a significant challenge. Similarly, the development and use of bio-based resins are crucial for reducing the carbon footprint of composite structures without compromising mechanical performance. Striking a balance between durability, cost, and environmental sustainability remains a key challenge. Future advancements should focus on creating formulations that meet stringent aerospace standards whilst addressing ecological concerns.

7.3. Environmental Impact

The evaluation of environmental factors such as temperature [145], humidity [146], and UV exposure is critical for understanding the long-term performance of composite components. These factors, inherent to the operational environment, can degrade the polymer matrix or even the matrix for natural and polymeric fibres, leading to reduced fibre–matrix adhesion, compromised laminate bonding, and diminished mechanical properties. Over time, since such degradation is already a known problem for general mechanical properties, it could also impact crashworthiness and complicate predictions of component reliability. This is especially significant because composite materials frequently exposed to sunlight, moisture, and temperature fluctuations are susceptible to these effects, requiring comprehensive analysis for improved durability and predictive modelling.

7.4. Geometric Innovations

Innovative structural designs, such as auxetic patterns, lattice frameworks, and multi-cell configurations, offer new opportunities to maximise energy absorption whilst minimising weight [147]. These geometries improve specific energy absorption and allow for tailored failure modes, which enhance crashworthiness. Additionally, advancements in additive manufacturing could significantly contribute to creating complex geometries that were previously difficult to achieve with traditional fabrication methods.

7.5. AI-Driven Predictive Modelling

The integration of artificial intelligence (AI) into crashworthiness research represents a transformative approach. AI-driven simulations enable real-time prediction and monitoring of structural performance during impacts, providing unmatched accuracy and efficiency. By combining machine learning algorithms with traditional modelling techniques, these tools can more accurately predict failure modes, deformation patterns, and energy absorption [148].

This approach significantly reduces the reliance on costly and time-consuming physical testing, accelerating design cycles whilst lowering development costs. Additionally, AI can optimise material selection and geometric configurations by identifying the most effective combinations for crashworthiness with greater speed and precision. This capability

supports the development of safer and more efficient aerospace structures, aligning with the industry's goals of innovation and sustainability.

7.6. Emerging Applications

The findings from crashworthiness research can be extended to emerging fields, such as urban air mobility (e.g., drones and eVTOL aircraft), space exploration, and the design of autonomous vehicles. These applications require lightweight, durable, and energy-absorbing materials to ensure safety and functionality in extreme conditions.

8. Conclusions

This manuscript has provided a comprehensive review of the crashworthiness of composite structures in the aerospace industry, with a focus on key aspects such as regulatory framework, effective parameters for component optimisation, and numerical simulation techniques.

In aerospace design, crashworthiness is critical for ensuring both structural integrity and passenger safety. Over the years, aerospace materials have evolved to meet stringent requirements for strength, weight efficiency, energy absorption, and durability. Whilst metallic materials initially dominated aircraft construction due to their strength and versatility, the industry has increasingly embraced advanced composite materials, which combine high performance with reduced weight, enhancing payload capacity, endurance, and fuel efficiency. Additionally, their superior energy absorption capabilities, driven by stable crushing behaviour and high SEA, make them ideal for crashworthy designs.

Regulatory bodies such as the FAA and EASA have played a crucial role in advancing safety standards. The increasing use of composites in modern vehicles has led to updates in regulations to better account for the properties of these materials. Experimental testing remains essential for assessing crashworthiness, with methods such as crush tests, impact towers, and sledge tests providing critical insights into energy absorption and failure modes under different conditions. However, numerical simulations complement experimental approaches by reducing the need for physical testing. Advanced modelling techniques address the different failure mechanisms of composites, such as fibre fracture and matrix cracking. Multiscale models (from macroscale to microscale) enable detailed and efficient analysis, whilst progressive failure models, continuum damage models, and non-local damage models capture material degradation with varying levels of fidelity and computational demand.

As urban air mobility, autonomous vehicles, and space exploration continue to expand, the demand for comprehensive crashworthiness assessments has increased. These initiatives drive the need for innovative research focused on achieving greater efficiency whilst minimising environmental impact. Future advancements integrating AI optimisation and predictive modelling offer exciting possibilities, including the development of novel structural designs and geometries that emphasise sustainability. This approach has the potential to overcome current limitations and meet the evolving requirements of crashworthy structures, paving the way for innovative, sustainable, and high-performance solutions.

Author Contributions: M.P.F.: conceptualisation, methodology, writing—original draft, and supervision; J.B.H.: resources, methodology, and writing—original draft; F.S.: resources, methodology, and writing—original draft; E.T.: conceptualisation, writing—review and editing, and funding acquisition. All authors have read and agreed to the published version of the manuscript.

Funding: This study was carried out within the MOST–Sustainable Mobility National Research Center and received funding from the European Union NextGenerationEU (PIANO NAZIONALE DI RIPRESA E RESILIENZA (PNRR)–MISSIONE 4 COMPONENTE 2, INVESTIMENTO 1.4–D.D. 1033 17/06/2022, CN00000023, CUP: J33C22001120001) and through the Italian Ministry of University and Research under PNRR-Mission 4 Component 1, Investment 4.1 "Extension of the number of PhD programmes and innovative PhD programmes for Public Administration and cultural heritage" and Investment 3.4 "Advanced university education and skills–Support to PhD programmes for digital and environmental transition". This manuscript reflects only the authors' views and opinions; neither the European Union nor the European Commission can be considered responsible for them.

Data Availability Statement: No new data were created or analysed in this study. Data sharing is not applicable to this article.

Conflicts of Interest: The authors declare no conflict of interest.

Abbreviations

The following abbreviations are used in this manuscript:

AC	Advisory Circular
AI	artificial intelligence
AMC	Acceptable Means of Compliance
CDM	continuum damage model
CE	Crush Efficiency
CF	carbon fibre
CFR	Code of Federal Regulations
CFRP	carbon fibre-reinforced plastic
CMH-17	Composite Materials Handbook-17
CZM	Cohesive Zone Model
EA	energy absorption
EASA	European Union Aviation Safety Agency
EPP	expanded polypropylene
FAA	Federal Aviation Administration
FE	finite element
GF	glass fibre
GFRP	glass fibre-reinforced plastic
KF	Kevlar fibre
KFRP	Kevlar fibre-reinforce plastic
NDM	non-local damage model
PAS	polyarylsulfone
PEK	polyetherketone
PEEK	polyetheretherketone
PEI	polyetherimide
PES	polyethersulfone
PI	polyimide
PFM	progressive failure model
SC	special condition
SMA	Shape Memory Allow
SEA	specific energy absorption
VCCT	Virtual Crack Closure Technique

References

1. Zimmnermann, R.E.; Merritt, N.A.; Lane, A.D.; Warrick, J.C.; Bolukbasi, A.O. *AD-A218 436—Aircraft Crash Survival Design Guide*; Simula Inc.: Phoenix, AZ, USA, 1989.
2. Singley, G.T. *US Army Crashworthiness Program*; Technical Report 810615; SAE Technical Papers; SAE International: Warrendale, PA, USA, 1981.

3. Jackson, K.E.; Fasanella, E.L.; Lyle, K.H. Crash Certification by Analysis—Are We There Yet? In Proceedings of the Annual Forum Proceedings—AHS International, Phoenix, AZ, USA, 9–11 May 2006; Volume 1, pp. 549–562.
4. European Union Aviation Safety Agency. *EASA's Regulatory Role: Increasing Safety, Environmental Protection and Enabling Innovation via Rulemaking*; European Union Aviation Safety Agency: Cologne, Germany, 2024.
5. European Union Aviation Safety Agency. *Certification Specifications and Acceptable Means of Compliance for Large Aeroplanes (CS-25)*; European Union Aviation Safety Agency: Cologne, Germany, 2023.
6. Federal Aviation Administration. *AC 25-17A—Transport Airplane Cabin Interiors Crashworthiness Handbook*; Federal Aviation Administration: Washington, DC, USA, 2009.
7. Mou, H.; Xie, J.; Feng, Z. Research Status and Future Development of Crashworthiness of Civil Aircraft Fuselage Structures: An Overview. *Prog. Aerosp. Sci.* **2020**, *119*, 100644. [CrossRef]
8. European Union Aviation Safety Agency. *Proposed Special Condition on "Crash Survivability for CFRP Fuselage" Applicable to Airbus A350-941*; European Union Aviation Safety Agency: Cologne, Germany, 2007.
9. Federal Aviation Administration. *Special Conditions: Boeing Model 787-8 Airplane; Crashworthiness*; Technical Report Docket No. NM368, Special Conditions No. 25-362-SC; US Department of Transportation Federal Aviation Administration: Washington, DC, USA, 2007.
10. Federal Aviation Administration. *Special Conditions: The Boeing Company Model 777 Series Airplanes; Passenger Seats with Pretensioner Restraint Systems*; Technical Report Docket No. FAA-2022-1740; Special Conditions No. 25-841-SC; US Department of Transportation Federal Aviation Administration: Washington, DC, USA, 2023.
11. European Union Aviation Safety Agency. *AMC 20-29 Composite Aircraft Structure—Easy Access Rules for Acceptable Means of Compliance for Airworthiness of Products, Parts and Appliances (AMC-20)*; European Union Aviation Safety Agency: Cologne, Germany, 2021.
12. Federal Aviation Administration. *Advisory Circular 20-107B. Composite Aircraft Structure*; US Department of Transportation Federal Aviation Administration: Washington, DC, USA, 2009.
13. Andrulonis, R.; Kiser, J.D. *CMH-17 Volume 5 Ceramic Matrix Composites*; Technical Report No. GRC-E-DAA-TN44028; American Society of Mechanical Engineers: New York, NY, USA, 2017.
14. ANC Committee on Aircraft Design Criteria. *Plastics for Aircraft ANC-17 Bulletin*; U.S. Army-Navy-Civil Committee on Aircraft Design Criteria, Civil Aeronautics Board: Washington, DC, USA, 1943.
15. ASTM ASTM Committee D30 Scope. Available online: https://www.astm.org/get-involved/technical-committees/committee-d30/scope-d30 (accessed on 27 December 2024).
16. SAE International. *CMH-17 Polymer Matrix Composites: Materials Usage, Design, and Analysis Revision G*; SAE International: Warrendale, PA, USA, 2012; ISBN 978-0-7680-7831-8.
17. Wade, B.; Deleo, F.; Feraboli, P.; Rassaian, M. Crushing of Composite Structures: Experiment and Simulation. In Proceedings of the 50th AIAA/ASME/ASCE/AHS/ASC Structures, Structural Dynamics, and Materials Conference, Palm Springs, CA, USA, 4–7 May 2009; American Institute of Aeronautics and Astronautics: Reston, VA, USA, 2009.
18. Farley, G.L. Energy-Absorption Capability and Scalability of Square Cross Section Composite Tube Specimens. *J. Am. Helicopter Soc.* **1989**, *34*, 59–62. [CrossRef]
19. Feraboli, P. Current Efforts in Standardization of Composite Materials Testing for Crashworthiness and Energy Absorption. In Proceedings of the Collection of Technical Papers—AIAA/ASME/ASCE/AHS/ASC Structures, Structural Dynamics and Materials Conference, Newport, RI, USA, 1–4 May 2006; Volume 10, pp. 7427–7444.
20. Vigna, L.; Calzolari, A.; Galizia, G.; Belingardi, G.; Paolino, D.S. Effect of Friction on a Crashworthiness Test of Flat Composite Plates. *Forces Mech.* **2022**, *6*, 100070. [CrossRef]
21. Feraboli, P.; Wade, B.; Deleo, F.; Rassaian, M. Crush Energy Absorption of Composite Channel Section Specimens. *Compos. Part A Appl. Sci. Manuf.* **2009**, *40*, 1248–1256. [CrossRef]
22. Jacob, G.C.; Fellers, J.F.; Simunovic, S.; Starbuck, J.M. Energy Absorption in Polymer Composites for Automotive Crashworthiness. *J. Compos. Mater.* **2002**, *36*, 813–850. [CrossRef]
23. David, M.; Johnson, A.F.; Voggenreiter, H. Analysis of Crushing Response of Composite Crashworthy Structures. *Appl. Compos. Mater.* **2013**, *20*, 773–787. [CrossRef]
24. Falzon, B.G. Computational Modelling of the Crushing of Carbon Fibre-Reinforced Polymer Composites. *Philos. Trans. R. Soc. A Math. Phys. Eng. Sci.* **2022**, *380*, 20210336. [CrossRef]
25. David, M.; Johnson, A.F. Effect of Strain Rate on the Failure Mechanisms and Energy Absorption in Polymer Composite Elements under Axial Loading. *Compos. Struct.* **2015**, *122*, 430–439. [CrossRef]
26. Mamalis, A.G.; Robinson, M.; Manolakos, D.E.; Demosthenous, G.A.; Ioannidis, M.B.; Carruthers, J. Crashworthy Capability of Composite Material Structures. *Compos. Struct.* **1997**, *37*, 109–134. [CrossRef]
27. Brighton, A.; Forrest, M.; Starbuck, M.; Erdman, D.; Fox, B. Strain Rate Effects on the Energy Absorption of Rapidly Manufactured Composite Tubes. *J. Compos. Mater.* **2009**, *43*, 2183–2200. [CrossRef]

28. Thornton, P.H.; Harwood, J.J.; Beardmore, P. Fiber-Reinforced Plastic Composites for Energy Absorption Purposes. *Compos. Sci. Technol.* **1985**, *24*, 275–298. [CrossRef]
29. Lausch, J.; Takla, M.; Schweiger, H.G. Crush Testing Approach for Flat-Plate Fibrous Materials. *Compos. B Eng.* **2020**, *200*, 108333. [CrossRef]
30. Jackson, K.; Morton, J.; Traffanstedt, C.; Boitnott, R. Scaling of Energy Absorbing Composite Plates. In Proceedings of the AHS, Annual Forum, 48th, Washington, DC, USA, 3–5 June 1992; Volume 2.
31. Lavoie, J.A.; Morton, J. *Design and Application of a Quasistatic Crush Test Fixture for Investigating Scale Effects in Energy Absorbing Composite Plates*; Master's thesis, Virginia Polytechnic Institute and State University: Blacksburg, VA, USA, 1993.
32. Feraboli, P. Development of a Modified Flat-Plate Test Specimen and Fixture for Composite Materials Crush Energy Absorption. *J. Compos. Mater.* **2009**, *43*, 1967–1990. [CrossRef]
33. Daniel, L.; Hogg, P.J.; Curtis, P.T. The Relative Effects of Through-Thickness Properties and Fibre Orientation on Energy Absorption by Continuous Fibre Composites. *Compos. B Eng.* **1999**, *30*, 257–266. [CrossRef]
34. Jacob, G.C.; Starbuck, J.M.; Fellers, J.F.; Simunovic, S.; Boeman, R.G. Crashworthiness of Various Random Chopped Carbon Fiber Reinforced Epoxy Composite Materials and Their Strain Rate Dependence. *J. Appl. Polym. Sci.* **2006**, *101*, 1477–1486. [CrossRef]
35. Engenuity Limited Equipment for Dynamic Testing. Available online: https://engenuity.net/techniques/equipment-software/equipment-for-dynamic-testing/ (accessed on 12 December 2024).
36. Fairfull, A.H.; Hul, D. Energy Absorption of Polymer Matrix Composite Structures: Frictional Effects. In *Structural Failure*; John Wiley & Sons: Hoboken, NJ, USA, 1989; pp. 255–279.
37. Vigna, L.; Calzolari, A.; Galizia, G.; Belingardi, G.; Paolino, D.S. Effect of Impact Speed and Friction on the In-Plane Crashworthiness of Composite Plates. *Procedia Struct. Integr.* **2021**, *33*, 623–629. [CrossRef]
38. Brimhall, T.J. Measurement of Static and Dynamic Friction Energy Absorption in Carbon/Vinyl Ester Composite. In Proceedings of the 6th Annual SPE Automotive Composites Conference 2006, Troy, MI, USA 12–14 September 2006; Volume 2, pp. 683–695.
39. Eshkoor, R.A.; Oshkovr, S.A.; Sulong, A.B.; Zulkifli, R.; Ariffin, A.K.; Azhari, C.H. Effect of Trigger Configuration on the Crashworthiness Characteristics of Natural Silk Epoxy Composite Tubes. *Compos. B Eng.* **2013**, *55*, 5–10. [CrossRef]
40. Browne, A.L.; Johnson, N.L. Dynamic Crush Tests Using a "Free-Flight" Drop Tower: Theory. *Exp. Tech.* **2002**, *26*, 43–46. [CrossRef]
41. Haluza, R.T.; Ruggeri, C.R.; Pereira, J.M.; Miller, S.G.; Bakis, C.E.; Koudela, K.L. Novel Crash Sled with a Translating Support Mass. *Exp. Mech.* **2022**, *62*, 715–728. [CrossRef]
42. Feraboli, P. Some Recommendations for Characterization of Composite Panels by Means of Drop Tower Impact Testing. *J. Aircraft* **2006**, *43*, 1710–1718. [CrossRef]
43. Link, T.M.; Grimm, J.S.; Link, T.M.; Grimm, J.S. *Axial Crash Testing of Advanced High Strength Steel Tubes*; Technical Report No. 2005-01-0836; SAE Technical Papers; SAE International: Warrendale, PA, USA, 2005. [CrossRef]
44. Liu, X.; Belkassem, B.; Jonet, A.; Lecompte, D.; Van Hemelrijck, D.; Pintelon, R.; Pyl, L. Experimental Investigation of Energy Absorption Behaviour of Circular Carbon/Epoxy Composite Tubes under Quasi-Static and Dynamic Crush Loading. *Compos. Struct.* **2019**, *227*, 111266. [CrossRef]
45. Berry, J.P.; Blears, J.; Grundy, J.D.; Keale, R.; Seddeon, B.; Snowdon, R.P.; Hull, D. Energy Absorption Composites Group Report 9. In *Department of Materials Science and Metallurgy*; University of Liverpool: Liverpool, UK, 1982.
46. Thornton, P.H.; Jeryan, R.A. Crash Energy Management in Composite Automotive Structures. *Int. J. Impact Eng.* **1988**, *7*, 167–180. [CrossRef]
47. Warrior, N.A.; Turner, T.A.; Robitaille, F.; Rudd, C.D. Effect of Resin Properties and Processing Parameters on Crash Energy Absorbing Composite Structures Made by RTM. *Compos. Part A Appl. Sci. Manuf.* **2003**, *34*, 543–550. [CrossRef]
48. Ramakrishna, S.; Hamada, H.; Maekawa, Z.; Sato, H. Energy Absorption Behavior of Carbon-Fiber-Reinforced Thermoplastic Composite Tubes. *J. Thermoplast. Compos. Mater.* **1995**, *8*, 323–344. [CrossRef]
49. Hamada, H.; Ramakrishna, S.; Satoh, H. Crushing Mechanism of Carbon Fibre/PEEK Composite Tubes. *Composites* **1995**, *26*, 749–755. [CrossRef]
50. Hamada, H.; Coppola, J.C.; Hull, D.; Maekawa, Z.; Sato, H. Comparison of Energy Absorption of Carbon/Epoxy and Carbon/PEEK Composite Tubes. *Composites* **1992**, *23*, 245–252. [CrossRef]
51. Ramírez, J.G.; Ghasemnejad, H. Z-Pinning Techniques to Improve Energy Absorption Capabilities of CFRP Tubular Structures. *Appl. Compos. Mater.* **2023**, *30*, 1529–1545. [CrossRef]
52. Rabiee, A.; Ghasemnejad, H. Effect of Stitching Pattern on Composite Tubular Strucutre Subjected to Quasi-Static Crushing. *Int. J. Mater. Metall. Eng.* **2016**, *10*, 1261–1265.
53. Falaschetti, M.P.; Rondina, F.; Maccaferri, E.; Mazzocchetti, L.; Donati, L.; Zucchelli, A.; Giorgini, L. Improving the Crashworthiness of CFRP Structures by Rubbery Nanofibrous Interlayers. *Compos. Struct.* **2023**, *311*, 116845. [CrossRef]

54. Kohlgrueber, D.; Kamoulakos, A. Validation of Numerical Simulation of Composite Helicopter Sub-Floor Structures Under Crash Loading. In Proceedings of the Annual Forum Proceedings—American Helicopter Society, Washington, DC, USA, 20–22 May 1998; American Helicopter Society: Washington, DC, USA, 1998; Volume 1, pp. 340–349.
55. Guo, K.; Liu, X.; Ren, Y.; Jiang, H. Experimental Study on Crashworthiness and Failure Mechanisms of Aeronautical Multi-Fibers Hybrid Composite Corrugated Structures with Carbon, Glass, Kevlar. *Aerosp. Sci. Technol.* **2023**, *142*, 108599. [CrossRef]
56. de Lemos Coutinho, L.; Abada, M.; Ibrahim, A.; Jung, S.J. Energy Absorption of CFRP Composite Thin-Walled Tubes with PVC Foam-Filled Cores. *Innov. Infrastruct. Solut.* **2022**, *7*, 168. [CrossRef]
57. Özsoy, M.İ.; Yalçın, M.M.; Yaren, M.F. Investigation on Quasi-Static Compression of Circular CFRP Tubes: Effect of EPP Foam Filling. *J. Braz. Soc. Mech. Sci. Eng.* **2023**, *45*, 442. [CrossRef]
58. Rondina, F.; Falaschetti, M.P.; Zavatta, N.; Donati, L. Numerical Simulation of the Compression Crushing Energy of Carbon Fiber-Epoxy Woven Composite Structures. *Compos. Struct.* **2023**, *303*, 116300. [CrossRef]
59. Sokolinsky, V.S.; Indermuehle, K.C.; Hurtado, J.A. Numerical Simulation of the Crushing Process of a Corrugated Composite Plate. *Compos. Part A Appl. Sci. Manuf.* **2011**, *42*, 1119–1126. [CrossRef]
60. Joosten, M.W.; Dutton, S.; Kelly, D.; Thomson, R. Experimental and Numerical Investigation of the Crushing Response of an Open Section Composite Energy Absorbing Element. *Compos. Struct.* **2011**, *93*, 682–689. [CrossRef]
61. Joosten, M.W.; Hirth, C.; Thomson, R.; Koerber, H. Effect of Environmental Conditions on the Failure Mechanisms and Energy Absorption of Open-Section Crush Elements under Quasi-Static Loading. *Compos. Struct.* **2019**, *209*, 747–753. [CrossRef]
62. Jiménez, M.A.; Miravete, A.; Larrodé, E.; Revuelta, D. Effect of Trigger Geometry on Energy Absorption in Composite Profiles. *Compos. Struct.* **2000**, *48*, 107–111. [CrossRef]
63. Troiani, E.; Donati, L.; Molinari, G.; Di Sante, R. Influence of Plying Strategies and Trigger Type on Crashworthiness Properties of Carbon Fiber Laminates Cured through Autoclave Processing. *Stroj. Vestn. J. Mech. Eng.* **2014**, *60*, 375–381. [CrossRef]
64. Hussein, R.D.; Ruan, D.; Lu, G.; Thomson, R. An Energy Dissipating Mechanism for Crushing Square Aluminium/CFRP Tubes. *Compos. Struct.* **2018**, *183*, 643–653. [CrossRef]
65. Ma, Y.; Jin, S.; Zhang, S. Effect of Trigger on Crashworthiness of Unidirectional Carbon Fibre Reinforced Polyamide 6 Composites. *Plast. Rubber Compos.* **2018**, *47*, 208–220. [CrossRef]
66. Huang, J.C.; Wang, X.W. Effect of the SMA Trigger on the Energy Absorption Characteristics of CFRP Circular Tubes. *J. Compos. Mater.* **2010**, *44*, 639–651. [CrossRef]
67. Lavoie, J.A.; Kellas, S. Dynamic Crush Tests of Energy-Absorbing Laminated Composite Plates. *Compos. Part A Appl. Sci. Manuf.* **1996**, *27*, 467–475. [CrossRef]
68. Bru, T.; Waldenström, P.; Gutkin, R.; Olsson, R.; Vyas, G.M. Development of a Test Method for Evaluating the Crushing Behaviour of Unidirectional Laminates. *J. Compos. Mater.* **2017**, *51*, 4041–4051. [CrossRef]
69. Falaschetti, M.P.; Birnie Hernández, J.; Semprucci, F.; Raimondi, L.; Serradimigni, D.; Troiani, E.; Donati, L. Analysis of the Crushing Behavior of Flat Composite Plates Produced by Sheet Molding Compound. In *Dynamic Response and Failure of Composite Materials. DRAF 2024*; Lecture Notes in Mechanical Engineering; Lopresto, V., Papa, I., Eds.; Springer: Cham, Switzerland, 2025; pp. 40–48.
70. Feraboli, P. Development of a Corrugated Test Specimen for Composite Materials Energy Absorption. *J. Compos. Mater.* **2008**, *42*, 229–256. [CrossRef]
71. Tan, W.; Falzon, B.G. Modelling the Crush Behaviour of Thermoplastic Composites. *Compos. Sci. Technol.* **2016**, *134*, 57–71. [CrossRef]
72. Deleo, F.; Wade, B.; Feraboli, P. Crashworthiness of Composite Structures: Experiment and Simulation. In Proceedings of the 11th Annual Automotive Composites Conference and Exhibition 2011, ACCE 2011, Troy, MI, USA, 13–15 September 2011; Society of Plastics Engineers -SPE-: Troy, MI, USA, 2012; pp. 68–715.
73. Jackson, A.; Dutton, S.; Gunnion, A.J.; Kelly, D. Investigation into Laminate Design of Open Carbon-Fibre/Epoxy Sections by Quasi-Static and Dynamic Crushing. *Compos. Struct.* **2011**, *93*, 2646–2654. [CrossRef]
74. Farley, G.L. The Effects of Crushing Speed on the Energy-Absorption Capability of Composite Tubes. *J. Compos. Mater.* **1991**, *25*, 1314–1329. [CrossRef]
75. Farley, G.L. Effect of Specimen Geometry on the Energy Absorption Capability of Composite Materials. *J. Compos. Mater.* **1986**, *20*, 390–400. [CrossRef]
76. Chiu, L.N.S.; Falzon, B.G.; Ruan, D.; Xu, S.; Thomson, R.S.; Chen, B.; Yan, W. Crush Responses of Composite Cylinder under Quasi-Static and Dynamic Loading. *Compos. Struct.* **2015**, *131*, 90–98. [CrossRef]
77. Mamalis, A.G.; Manolakos, D.E.; Ioannidis, M.B.; Papapostolou, D.P. On the Response of Thin-Walled CFRP Composite Tubular Components Subjected to Static and Dynamic Axial Compressive Loading: Experimental. *Compos. Struct.* **2005**, *69*, 407–420. [CrossRef]
78. Liu, Q.; Ou, Z.; Mo, Z.; Li, Q.; Qu, D. Experimental Investigation into Dynamic Axial Impact Responses of Double Hat Shaped CFRP Tubes. *Compos. B Eng.* **2015**, *79*, 494–504. [CrossRef]

79. Garattoni, F. Crashworthiness and Composite Materials: Development of an Experimental Test Method for the Energy Absorption Determination and Implementation of the Relative Numerical Model. Ph.D. Thesis, University of Bologna, Bologna, Italy, 2011.
80. Feraboli, P.; Deleo, F.; Garattoni, F. Efforts in the Standardization of Composite Materials Crashworthiness Energy Absorption. In Proceedings of the 22nd Technical Conference of the American Society for Composites 2007, Seattle, WA, USA, 17–19 September 2007; American Society for Composites: Seattle, WA, USA, 2007; pp. 741–759.
81. Hu, D.; Zhang, C.; Ma, X.; Song, B. Effect of Fiber Orientation on Energy Absorption Characteristics of Glass Cloth/Epoxy Composite Tubes under Axial Quasi-Static and Impact Crushing Condition. *Compos. Part A Appl. Sci. Manuf.* **2016**, *90*, 489–501. [CrossRef]
82. Paz, J.; Díaz, J.; Romera, L. Analytical and Numerical Crashworthiness Uncertainty Quantification of Metallic Thin-Walled Energy Absorbers. *Thin-Walled Struct.* **2020**, *157*, 107022. [CrossRef]
83. Abbasi, M.; Reddy, S.; Ghafari-Nazari, A.; Fard, M. Multiobjective Crashworthiness Optimization of Multi-Cornered Thin-Walled Sheet Metal Members. *Thin-Walled Struct.* **2015**, *89*, 31–41. [CrossRef]
84. El-Hage, H.; Mallick, P.K.; Zamani, N. A Numerical Study on the Quasi-Static Axial Crush Characteristics of Square Aluminum–Composite Hybrid Tubes. *Compos. Struct.* **2006**, *73*, 505–514. [CrossRef]
85. Spearing, S.M.; Lagace, P.A.; Mcmanus, H.L.N. On the Role of Lengthscale in the Prediction of Failure of Composite Structures: Assessment and Needs. *Appl. Compos. Mater.* **1998**, *5*, 139–149. [CrossRef]
86. Caporale, A.; Luciano, R.; Sacco, E. Micromechanical Analysis of Interfacial Debonding in Unidirectional Fiber-Reinforced Composites. *Comput. Struct.* **2006**, *84*, 2200–2211. [CrossRef]
87. Maligno, A.R.; Warrior, N.A.; Long, A.C. Effects of Interphase Material Properties in Unidirectional Fibre Reinforced Composites. *Compos. Sci. Technol.* **2010**, *70*, 36–44. [CrossRef]
88. Ladevèze, P.; Allix, O.; Deü, J.F.; Lévêque, D. A Mesomodel for Localisation and Damage Computation in Laminates. *Comput. Methods Appl. Mech. Eng.* **2000**, *183*, 105–122. [CrossRef]
89. Feld, N.; Allix, O.; Baranger, E.; Guimard, J.M. A Micromechanics-Based Mesomodel for Unidirectional Laminates in Compression up to Failure. *J. Compos. Mater.* **2012**, *46*, 2893–2909. [CrossRef]
90. Allix, O.; Deü, J.-F. Delayed-Damage Modelling for Fracture Prediction of Laminated Composites under Dynamic Loading. *Eng. Trans.* **1997**, *45*, 29–46. [CrossRef]
91. Guillon, D.; Rivallant, S.; Barrau, J.; Petiot, C.; Thevenet, P.; Malherbe, B. Experimental and Numerical Study of the Splaying Mode Crush of CFRP Laminates. In Proceedings of the ICCM International Conferences on Composite Materials, Edinburgh, UK, 27–31 July 2009.
92. Hashin, Z. Failure Criteria for Unidirectional Fiber Composites. *J. Appl. Mech. Trans. ASME* **1980**, *47*, 329–334. [CrossRef]
93. Chang, F.K.; Chang, K.Y. A Progressive Damage Model for Laminated Composites Containing Stress Concentrations. *J. Compos. Mater.* **2016**, *21*, 834–855. [CrossRef]
94. Puck, A.; Schürmann, H. Failure Analysis of FRP Laminates by Means of Physically Based Phenomenological Models. *Compos. Sci. Technol.* **2002**, *62*, 1633–1662. [CrossRef]
95. Dávila, C.G.; Camanho, P.P.; Rose, C.A. Failure Criteria for FRP Laminates. *J. Compos. Mater.* **2005**, *39*, 323–345. [CrossRef]
96. Pinho, S.T.; Dávila, C.G.; Camanho, P.P.; Iannucci, L.; Robinson, P. *Failure Models and Criteria for FRP Under In-Plane or Three-Dimensional Stress States Including Shear Non-Linearity*; NASA Langley Research Center: Hampton, VA, USA, 2005.
97. Hashin, Z.; Rotem, A. A Fatigue Failure Criterion for Fiber Reinforced Materials. *J. Compos. Mater.* **1973**, *7*, 448–464. [CrossRef]
98. Cuntze, R.G.; Freund, A. The Predictive Capability of Failure Mode Concept-Based Strength Criteria for Multidirectional Laminates. *Compos. Sci. Technol.* **2004**, *64*, 343–377. [CrossRef]
99. Chang, F.K.; Lessard, L.B. Damage Tolerance of Laminated Composites Containing an Open Hole and Subjected to Compressive Loadings: Part I—Analysis. *J. Compos. Mater.* **1991**, *25*, 2–43. [CrossRef]
100. Shahid, I.; Chang, F.K. An Accumulative Damage Model for Tensile and Shear Failures of Laminated Composite Plates. *J. Compos. Mater.* **1995**, *29*, 926–981. [CrossRef]
101. Ladevèze, P. A Damage Computational Method for Composite Structures. *Comput. Struct.* **1992**, *44*, 79–87. [CrossRef]
102. Lee, J.D. Three Dimensional Finite Element Analysis of Damage Accumulation in Composite Laminate. *Comput. Struct.* **1982**, *15*, 335–350. [CrossRef]
103. Christensen, R.M. Stress Based Yield/Failure Criteria for Fiber Composites. *Int. J. Solids Struct.* **1997**, *34*, 529–543. [CrossRef]
104. Tsai, S.W.; Wu, E.M. A General Theory of Strength for Anisotropic Materials. *J. Compos. Mater.* **1971**, *5*, 58–80. [CrossRef]
105. Yamada, S.E.; Sun, C.T. Analysis of Laminate Strength and Its Distribution. *J. Compos. Mater.* **1978**, *12*, 275–284. [CrossRef]
106. Tong, L. An Assessment of Failure Criteria to Predict the Strength of Adhesively Bonded Composite Double Lap Joints. *J. Reinf. Plast. Compos.* **1997**, *16*, 698–713. [CrossRef]
107. Benzeggagh, M.L.; Kenane, M. Measurement of Mixed-Mode Delamination Fracture Toughness of Unidirectional Glass/Epoxy Composites with Mixed-Mode Bending Apparatus. *Compos. Sci. Technol.* **1996**, *56*, 439–449. [CrossRef]

108. Camanho, P.P.; Davila, C.G. *Mixed-Mode Decohesion Finite Elements for the Simulation of Delamination in Composite Materials*; Technical Report No. 211737; NASA Langley Research Center: Hampton, VA, USA, 2002.
109. Borg, R.; Nilsson, L.; Simonsson, K. Simulation of Delamination in Fiber Composites with a Discrete Cohesive Failure Model. *Compos. Sci. Technol.* **2001**, *61*, 667–677. [CrossRef]
110. Qiu, Y.; Crisfield, M.A.; Alfano, G. An Interface Element Formulation for the Simulation of Delamination with Buckling. *Eng. Fract. Mech.* **2001**, *68*, 1755–1776. [CrossRef]
111. Hamada, H.; Ramakrishna, S. A FEM Method for Prediction of Energy Absorption Capability of Crashworthy Polymer Composite Materials. *J. Reinf. Plast. Compos.* **1997**, *16*, 226–242. [CrossRef]
112. Talreja, R. Damage Characterization. In *Composite Materials Series*; Elsevier: Amsterdam, The Netherlands, 1991; Volume 4, pp. 79–103.
113. Johnson, A.F.; Pickett, A.K.; Rozycki, P. Computational Methods for Predicting Impact Damage in Composite Structures. *Compos. Sci. Technol.* **2001**, *61*, 2183–2192. [CrossRef]
114. Ladevèze, P.; Allix, O.; Gornet, L.; Lévêque, D.; Perret, L. A Computational Damage Mechanics Approach for Laminates: Identification and Comparison with Experimental Results. *Stud. Appl. Mech.* **1998**, *46*, 481–500. [CrossRef]
115. Maimí, P.; Camanho, P.P.; Mayugo, J.A.; Dávila, C.G. A Continuum Damage Model for Composite Laminates: Part II—Computational Implementation and Validation. *Mech. Mater.* **2007**, *39*, 909–919. [CrossRef]
116. Matzenmiller, A.; Lubliner, J.; Taylor, R.L. A Constitutive Model for Anisotropic Damage in Fiber-Composites. *Mech. Mater.* **1995**, *20*, 125–152. [CrossRef]
117. Williams, K.V.; Vaziri, R.; Poursartip, A. A Physically Based Continuum Damage Mechanics Model for Thin Laminated Composite Structures. *Int. J. Solids Struct* **2003**, *40*, 2267–2300. [CrossRef]
118. McGregor, C.; Zobeiry, N.; Vaziri, R.; Poursartip, A. A Constitutive Model for Progressive Compressive Failure of Composites. *J. Compos. Mater.* **2008**, *42*, 2687–2716. [CrossRef]
119. McGregor, C.J.; Vaziri, R.; Poursartip, A.; Xiao, X. Simulation of Progressive Damage Development in Braided Composite Tubes under Axial Compression. *Compos. Part A Appl. Sci. Manuf.* **2007**, *38*, 2247–2259. [CrossRef]
120. Pineda, E.J.; Waas, A.M. Numerical Implementation of a Multiple-ISV Thermodynamically-Based Work Potential Theory for Modeling Progressive Damage and Failure in Fiber-Reinforced Laminates. *Int. J. Fract.* **2013**, *182*, 93–122. [CrossRef]
121. Bažant, Z.P.; Oh, B.H. Crack Band Theory for Fracture of Concrete. *Matériaux Constr.* **1983**, *16*, 155–177. [CrossRef]
122. Bažant, Z.P.; Pijaudier-Cabot, G. Nonlocal Continuum Damage, Localization Instability and Convergence. *J. Appl. Mech.* **1988**, *55*, 287–293. [CrossRef]
123. Rabczuk, T.; Belytschko, T. A Three-Dimensional Large Deformation Meshfree Method for Arbitrary Evolving Cracks. *Comput. Methods Appl. Mech. Eng.* **2007**, *196*, 2777–2799. [CrossRef]
124. Lorentz, E.; Andrieux, S. A Variational Formulation for Nonlocal Damage Models. *Int. J. Plast.* **1999**, *15*, 119–138. [CrossRef]
125. Guguin, G.; Allix, O.; Gosselet, P.; Guinard, S. Nonintrusive Coupling of 3D and 2D Laminated Composite Models Based on Finite Element 3D Recovery. *Int. J. Numer. Methods Eng.* **2014**, *98*, 324–343. [CrossRef]
126. Fleming, D.C. Delamination Modeling of Composites for Improved Crash Analysis. *J. Compos. Mater.* **2001**, *35*, 1777–1792. [CrossRef]
127. Rybicki, E.F.; Kanninen, M.F. A Finite Element Calculation of Stress Intensity Factors by a Modified Crack Closure Integral. *Eng. Fract. Mech.* **1977**, *9*, 931–938. [CrossRef]
128. Farley, G.L.; Jones, R.M. Prediction of the Energy-Absorption Capability of Composite Tubes. *J. Compos. Mater.* **1992**, *26*, 388–404. [CrossRef]
129. Shi, D.; Xiao, X. A New Shell-Beam Element Modeling Method and Its Use in Crash Simulation of Triaxial Braided Composites. *Compos. Struct.* **2017**, *160*, 792–803. [CrossRef]
130. Falaschetti, M.P.; Rondina, F.; Zavatta, N.; Troiani, E.; Donati, L. Effective Implementation of Numerical Models for the Crashworthiness of Composite Laminates. *Eng. Fail. Anal.* **2024**, *160*, 108196. [CrossRef]
131. Riccio, A.; Saputo, S.; Sellitto, A.; Di Caprio, F. On the Crashworthiness Behaviour of a Composite Fuselage Sub-Floor Component. *Compos. Struct.* **2020**, *234*, 111662. [CrossRef]
132. Feraboli, P.; Wade, B.; Deleo, F.; Rassaian, M.; Higgins, M.; Byar, A. LS-DYNA MAT54 Modeling of the Axial Crushing of a Composite Tape Sinusoidal Specimen. *Compos. Part A Appl. Sci. Manuf.* **2011**, *42*, 1809–1825. [CrossRef]
133. Raponi, E.; Fiumarella, D. Experimental Analysis and Numerical Optimization of a Thermoplastic Composite in Crashworthiness. *IOP Conf. Ser. Mater. Sci. Eng.* **2021**, *1038*, 012030. [CrossRef]
134. Perfetto, D.; De Luca, A.; Lamanna, G.; Chiariello, A.; Di Caprio, F.; Di Palma, L.; Caputo, F. Drop Test Simulation and Validation of a Full Composite Fuselage Section of a Regional Aircraft. *Procedia Struct. Integr.* **2018**, *12*, 380–391. [CrossRef]
135. Caputo, F.; Lamanna, G.; Perfetto, D.; Chiariello, A.; Di Caprio, F.; Di Palma, L. Experimental and Numerical Crashworthiness Study of a Full-Scale Composite Fuselage Section. *AIAA J.* **2021**, *59*, 700–718. [CrossRef]

136. Manzo, M.; Perfetto, D.; Caputo, F.; Di Palma, L.; Chiariello, A.; Waimer, M. A Crashworthiness Optimisation Procedure for the Design of Full-Composite Fuselage Section. *IOP Conf. Ser. Mater. Sci. Eng.* **2021**, *1038*, 012058. [CrossRef]
137. Xiao, X.; McGregor, C.; Vaziri, R.; Poursartip, A. Progress in Braided Composite Tube Crush Simulation. *Int. J. Impact Eng.* **2009**, *36*, 711–719. [CrossRef]
138. Jiang, H.; Ren, Y.; Gao, B. Research on the Progressive Damage Model and Trigger Geometry of Composite Waved Beam to Improve Crashworthiness. *Thin-Walled Struct.* **2017**, *119*, 531–543. [CrossRef]
139. Ladeveze, P.; LeDantec, E. Damage Modelling of the Elementary Ply for Laminated Composites. *Compos. Sci. Technol.* **1992**, *43*, 257–267. [CrossRef]
140. Haluza, R.T.; Goldberg, R.K.; Ricks, T.M.; Pereira, J.M.; Koudela, K.L.; Bakis, C.E. Modeling Dynamic Crush Behavior of Carbon Fiber Reinforced Polymer Composite Structures Using MAT213. *Compos. Struct.* **2024**, *338*, 118063. [CrossRef]
141. Luo, H.; Yan, Y.; Zhang, T.; He, Z.; Wang, S. Progressive Failure Numerical Simulation and Experimental Verification of Carbon-Fiber Composite Corrugated Beams under Dynamic Impact. *Polym. Test* **2017**, *63*, 12–24. [CrossRef]
142. Jiang, H.; Ren, Y.; Gao, B.; Xiang, J.; Yuan, F.G. Design of Novel Plug-Type Triggers for Composite Square Tubes: Enhancement of Energy-Absorption Capacity and Inducing Failure Mechanisms. *Int. J. Mech. Sci.* **2017**, *131–132*, 113–136. [CrossRef]
143. Ren, Y.; Jiang, H.; Liu, Z. Evaluation of Double- and Triple-Coupled Triggering Mechanisms to Improve Crashworthiness of Composite Tubes. *Int. J. Mech. Sci.* **2019**, *157–158*, 1–12. [CrossRef]
144. Hamada, H.; Ramakrishna, S.; Hamada, R.; Ramakrishna, H. *Comparison of Static and Impact Energy Absorption of Carbon Fiber/PEEK Composite Tubes*; American Society for Testing and Materials: West Conshohocken, PA, USA, 1996.
145. Zavatta, N.; Rondina, F.; Falaschetti, M.P.; Donati, L. Effect of Thermal Ageing on the Mechanical Strength of Carbon Fibre Reinforced Epoxy Composites. *Polymers* **2021**, *13*, 2006. [CrossRef] [PubMed]
146. Falaschetti, M.P.; Scafé, M.; Zavatta, N.; Troiani, E. Hygrothermal Ageing Influence on BVI-Damaged Carbon/Epoxy Coupons under Compression Load. *Polymers* **2021**, *13*, 2038. [CrossRef]
147. Franzosi, P.; Colamartino, I.; Giustina, A.; Anghileri, M.; Boniardi, M. Crashworthiness of Additively Manufactured Auxetic Lattices: Repeated Impacts and Penetration Resistance. *Materials* **2024**, *17*, 186. [CrossRef] [PubMed]
148. Laban, O.; Gowid, S.; Mahdi, E.; Musharavati, F. Experimental Investigation and Artificial Intelligence-Based Modeling of the Residual Impact Damage Effect on the Crashworthiness of Braided Carbon/Kevlar Tubes. *Compos. Struct.* **2020**, *243*, 112247. [CrossRef]